Marine Pollution Bulletin 175 (2022) 113393

Contents lists available at ScienceDirect

Marine Pollution Bulletin

journal homepage: www.elsevier.com/locate/marpolbul

Quantitative assessment of two oil-in-ice surface drift algorithms

Victor de Aguiar [a,b,*], Knut-Frode Dagestad [a], Lars Robert Hole [a,**], Knut Barthel [c]

[a] Norwegian Meteorological Institute, Allegt. 70, 5007 Bergen, Norway
[b] Department of Physics and Technology, UiT The Arctic University of Norway, Tromsø, Norway
[c] Geophysical Institute, University of Bergen, Bergen, Norway

ARTICLE INFO

Keywords:
Oil in ice
OpenDrift
Oil drift modeling
Oil trajectory modeling

ABSTRACT

The ongoing reduction in extent and thickness of sea ice in the Arctic might result in an increase of oil spill risk due to the expansion of shipping activity and oil exploration shift towards higher latitudes. This work assessed the response of two oil-in-ice surface drift models implemented in an open-source Lagrangian framework. By considering two numerical modeling experiments, our main finding indicates that the drift models provide fairly similar outputs when forced by the same input. It was also found that using higher resolution ice-ocean model does not imply better results. We highlight the role of sea ice in the spread, direction and distance traveled by the oil. The skill metric seems to be sensitive to the drift location, and drift model re-initialization is required to avoid forecast deterioration and ensure the accurate tracking of oil slicks in real operations.

1. Introduction

Oil has undoubtedly been an intrinsic character of our society over the last 100+ years. According to BP's World Energy 2019 report (British Petroleum, 2019), oil represents about 34% of the world total primary energy consumption and it is foreseen that it will continue being the major source of energy in the near future (Canada's Oil &amp and Natural Gas Producers, 2018). Estimations indicate that the oil and gas industry represented approximately 3.8% of the global economy in 2019. Only in the U.S., the oil and gas industry employed almost 900,000 professionals in this same year (Furnans et al., 2020).

Oil spill releases in the marine environment have been observed since the beginning of the 20th century and arose as a major concern in the 1960s as a result of the development of supertanker ships, offshore installations and oil exploration over continental shelves (Carpenter, 2019). Since then, large accidents (*e.g. Amoco Cadiz*, France - 1978; *Deepwater Horizon*, USA - 2010) have released massive amounts of oil in the ocean, directly impacting fish stocks, bird colonies and human resources. The Convention for the Protection of the Marine Environment of the North-East Atlantic (OSPAR) reported that more than 1350 offshore operational installations were present in the maritime zone under their jurisdiction (OSPAR Commission, 2021). The same commission reported that 4119 t of oil were discharged and spilled in the North Sea in 2017, being Norway responsible for about 40% of the spillage (OSPAR Commission, 2017, Table 5e).

In addition to the current oil-related operations, it is estimated that over 7800 sunken ships from World War II lie on the seafloor, of which 124 of them lie in the Arctic (Monfils, 2005). Since such shipwrecks have been underwater for more than 70 years, corrosion could make the steel structures fragile and ultimately cause oil leaks. This potential risk of oil pollution in ice-covered waters comes on the top of a crescent shipping activity and interest in oil exploration in the Arctic region. The Norwegian Petroleum Directorate (NPD), for example, estimates that about half of the total petroleum resources in Norwegian waters are still left to be discovered, with around 40% of that being located in the northern Barents Sea (The Norwegian Petroleum Directorate, 2018), close to the sea ice edge.

Simultaneously to this increase in resource interests, the ongoing reductions in sea ice extension (Serreze et al., 2007) and thickness (Wadhams and Davis, 2000) have also allowed the intensification of shipping activities in the Arctic region. The Northern Sea Route (NSR), for example, a shipping lane defined between Novaya Zemlya and the Bering Strait, transported 31.5 million tons of goods in 2019, 56.7% more than in 2018. A total of 143 billions of private investments is required to achieve the Kremlin's ultimate goal of 80 million tons of goods transported in the NSR by 2024 and 90 million tons by 2030.

* Correspondence to: V. de Aguiar, Norwegian Meteorological Institute, Allegt. 70, 5007 Bergen, Norway.
** Corresponding author.
E-mail addresses: victorm@met.no, victor.d.aguiar@uit.no (V. de Aguiar), knutfd@met.no (K.-F. Dagestad), lrh@met.no (L.R. Hole), knut.barthel@uib.no (K. Barthel).

https://doi.org/10.1016/j.marpolbul.2022.113393
Received 24 September 2021; Received in revised form 17 January 2022; Accepted 22 January 2022
Available online 4 February 2022

Even though the number of confirmed oil slicks and large oil spills (>700 t) have decreased over the years (Carpenter, 2019; The International Tanker Owners Pollution Federation, 2020), the risks associated with oil exploration and transportation are inherent to such activities and therefore research efforts have been made to improve our knowledge about the processes involved in the weathering and transport of oil in the ocean. Large oil-in-ice studies started by the middle of the 1970s with the Canadian Government Beaufort Project (*e.g.* Wilkinson et al., 2017) and a series of laboratory (Cox and Schultz, 1981; Singsaas et al., 2020) and field experiments have been conducted since then (Ross and Dickins, 1987; Sørstrøm et al., 2010). Buist et al. (2013) presents a literature review covering around 60 experimental or accidental oil spills located in ice-covered waters.

As a rule-of-thumb dated from the 1970s and further supported by theoretical arguments (Venkatesh et al., 1990) and field experiments (Sørstrøm et al., 2010), the surface drift of oil spilled in a sea ice covered ocean depends on the sea ice concentration (C). Oil tends to drift as in open waters when C is low (<30%) and with the sea ice field for high sea ice concentration values ($C \geq 80\%$). It is still not well established how the surface drift of oil behaves in the medium ranges of ice concentration ($30\% < C < 80\%$). However, various approaches have been proposed. (French-McCay et al., 2018), for example, considered that oil travels with the ice field even in this intermediate interval whereas (Nordam et al., 2019a) and (Arneborg et al., 2017), both described in Section 2, presented a linear deterministic and linear probabilistic transition, respectively.

Trites et al. (1986) considered different wind drag coefficients for sea ice (1%) and open water (3%) for modeling the drift of oil released during the *Kurdistan* cargo accident in Nova Scotia, Canada. No sea ice concentration information was explicitly provided for distinguishing the thresholds which these coefficient values should be applied, but the authors highlight however the role of accurate atmospheric-ocean data for short-term forecast for accurate trajectory modeling. The pioneer OILBRICE (Oil spill in Broken Ice) model developed by Venkatesh et al. (1990), considers that the surface drift of oil is entirely dictated by sea ice velocities when C is greater than 30%. The proposed model was evaluated using field observations obtained by Ross and Dickins (1987). Although the main focus of their study was the spreading of oil under ice conditions, the researchers reported promising modeled oil drift results despite the small amount of data for analysis.

The Norwegian Foundation for Scientific and Industrial Research (SINTEF) developed and maintains the trajectory, fate and response Oil Spill Contingency And Response (OSCAR) (Reed et al., 1999). Nordam et al. (2019a) used OSCAR to simulate the oil slick trajectory from an oil-in-ice field experiment in the Barents Sea marginal ice zone (reported sea ice concentration between 70%–90%) in 2009 (Sørstrøm et al., 2010). Good agreement between modeled and observed trajectories was reported, and the study highlighted the importance of considering sea ice rheology in the ice models instead of a simple sea ice-free drift approach.

The Spill Impact Model Application (SIMAP)/OIL and Spill Impact MAPping (OILMAP) software, developed and maintained by the RPS ASA Group, was also used to simulate field trials in Barents Sea marginal ice zone (Reed and Aamo, 1994), with sea ice concentration varying between 60% and 90%. The authors report good agreement between the observed oil slick and trajectories when the wind drift factor and turning angle were tuned according to the wind intensity and direction. SIMAP was also applied to simulate hypothetical oil spills from different scenarios (well blowouts, sub-sea pipeline leak or shipping accident) in the Beaufort Sea under sea ice conditions (Gearon et al., 2014). The results indicate profound effects of the sea ice on the oil weathering and transport. According to the authors, oil spread less when located in sea ice than in open waters and weathering processes are slowed. The authors also highlighted possible difficulties in clean up operations due to the presence of sea ice.

The Oil-MARS (Oil Spill Model for the Arctic Seas), developed at the Arctic and Antarctic Research Institute (AARI), assumes that oil will be transported with the ice field in regions where $C > 50\%$ only if the sea ice drift velocity is greater than the oil slick velocity (Stanovoy et al., 2012). The authors used Oil-MARS to simulate a hypothetical oil spill in the Gulf of Finland during heavy ice conditions, but no quantitative evaluations were done.

International cooperation initiatives have been established to improve the knowledge, models performance and response capabilities. Together with the Danish Maritime Safety Administration (DAMSA), SMHI maintains the Seatrack Web, an internet based software used to simulate oil spills and to support response measures in the Baltic Sea and part of the North Sea (Ambjorn, 2008; Kostianoy et al., 2008). Atmospheric forcing in Seatrack Web is incorporated from the HIgh Resolution Limited Area Model (HIRLAM) and ocean currents are obtained from the HIgh Resolution Operational Model for the Baltic (HIROMB). Arneborg et al. (2017) used Seatrack Web to reproduce the oil spill in the Baltic Sea in 2006 caused by the sinking of the Dominican-registered cargo ship Runner 4.

In addition, the OILSPILL project (Enhancing oil spill response capability in the Baltic Sea Region, 2019), composed by research institutes from Finland, Latvia, Denmark, Estonia, Lithuania and other countries, aims to organize oil spill combating in coastal areas in the Baltic Sea region by training volunteers and identifying cross-border legal requirements. The Center for Spills and Environmental Hazards from the University of New Hampshire has also been promoting workshops to experts under the Arctic Spill Modeling flag to discuss the current capability, flaws and possible improvements in oil spill modeling and detection under sea ice conditions. Further information can be found at https://crrc.unh.edu/workshop/AMSM_virtual_2020. A thorough review of oil fate and transport in ice conditions can be found in Drozdowski et al. (2011); Fingas and Hollebone (2014); Afenyo et al. (2016).

Oil-in-ice drift models, such as the ones described above, have been extensively used over the years by the community. Nonetheless, these are usually commercial softwares, and when free of charge, the source code is not open for modifications. Since oil slicks can travel long distances from its releasing point, large accidents might cross legal borders and pose international threats. Authorities have short time windows to plan the response countermeasures and this coordination could be facilitated and widely improved if the access to the modeling tools was simpler. In addition, no studies conducted so far compared the outputs of two different oil-in-ice drift models under a same set of simulations. This work intends to fill in these two gaps through the implementation, evaluation and comparison of two oil-in-ice drift algorithms using OpenDrift (Dagestad et al., 2018), an open-source Lagrangian particle tracking framework.

This article is structured as follows: Section 2 presents the OpenDrift framework, the two oil-in-ice drift models implemented, the data sets used for the simulated trajectories evaluation, the atmospheric and ocean-ice models used to force the virtual particles and the metrics used to assess the simulations. Section 3 presents the results obtained in the numerical modeling experiments and these are discussed in Section 4. Finally, Section 5 synthesizes the study and presents suggestions for further studies.

2. Methods and data

2.1. The oil drift model – OpenOil

The open-source Lagrangian particle tracking framework OpenDrift (Dagestad et al., 2018) was used in this work. Coded in Python and made available at https://opendrift.github.io, OpenDrift contains different modules, including an oil spill drift and fate model called OpenOil (Röhrs et al., 2018). Composed by sub-modules that describe the different transport and weathering processes, OpenOil uses tabulated oil information provided by the Norwegian Clean Seas Association for

Operating Companies (NOFO) and is also linked to the ADIOS oil library used by PyGNOME (https://github.com/NOAA-ORR-ERD/PyGnome), the National Atmospheric and Ocean Administration (NOAA) oil model.

For the horizontal drift, OpenOil includes the sum of four terms which are added linearly: 1) advection with ocean current, 2) surface elements are moved with a fraction of the wind speed, by default 2%, 3) elements are also moved by the Stokes drift, either taken from a wave model, or, as in this study, parameterized from the wind. The calculated surface Stokes drift is reduced with depth in the ocean according to Breivik et al. (2016), and 4) finally, a random walk term is added, corresponding to a diffusivity prescribed by the user. In the vertical, three different processes are considered: 1) surface oil may be entrained by breaking waves as parameterized by Li et al. (2017), 2) entrained oil droplets are prescribed a radius also according to Li et al. (2017), based on the oil properties as calculated with the NOAA ADIOS module, and 3) vertical mixing and buoyancy (with possibly resurfacing) is based on a random walk scheme described in Nordam et al. (2019b). Further details about the OpenOil physics are given in Röhrs et al. (2018) and Brekke et al. (2021).

OpenDrift is used by Norwegian state agencies (*e.g.* The Clean Seas Association for Operating Companies, NOFO, and the Norwegian Coastal Administration) for oil spill response plans and search-and-rescue operations. Furthermore, OpenOil was successfully employed in the Gulf of Mexico to reproduce the Deep Horizon Oil Spill (Hole et al., 2019), to investigate the role of ocean dynamics on the transport of hydrocarbons in the Straits of Florida (Androulidakis et al., 2020) and on the evaluation of potential of oil spills around Cuba (Hole et al., 2021).

2.2. Oil-in-ice drift models

In the previous OpenOil versions, oil-in-ice interactions were restricted to particles being deactivated when they reached a certain sea ice concentration threshold. The two oil-in-ice models implemented and evaluated in this study were proposed by Arneborg et al. (2017) and Nordam et al. (2019a), and are briefly described below.

As mentioned in Section 1, the horizontal surface drift of oil in sea ice covered areas may be described by the "30/80" approach. Based on this rule-of-thumb, Nordam et al. (2019a) proposed that the oil velocity ($\mathbf{v}_{oil}$) is composed as a combination of sea ice velocities ($\mathbf{v}_{ice}$), ocean currents ($\mathbf{v}_{water}$) and a wind factor ($\mathbf{f}_w$ $\mathbf{v}_{wind}$), weighted by κ_{ice}, a coefficient dependent on the sea ice concentration (C), as follows:

$$v_{oil} = \kappa_{ice} v_{ice} + (1 - \kappa_{ice})(v_{water} + f_w v_{wind}) \tag{1}$$

where

$$\kappa_{ice} \begin{cases} 0, & \text{if } C < 30\% \\ \dfrac{C - 30\%}{80\% - 30\%}, & \text{if } 30\% \le C < 80\% \\ 1, & \text{if } C \ge 80\% \end{cases}$$

Arneborg et al. (2017) presented a probabilistic approach in the interval 30% ≤ C < 80%. The probability, given by Eq. (2), of a particle changing its state from *free* → *attached* (to the sea ice), or *attached* → *free*, is based on the change of the particles state and of sea ice concentration values from a previous (C_1) to the current (C_2) time step.

$$P(free \rightarrow attached) \begin{cases} \dfrac{f(C_1) - f(C_2)}{f(C_1)}, & C_2 > C_1 \\ 0, & C_2 < C_1 \end{cases}, \tag{2}$$

where $f(C)$ is the fraction of particles in the free state at a given sea ice concentration C. If $C_1 > C_2$, none of particles will get attached to the sea ice, but they might start moving freely and this probability is given by:

$$P(attached \rightarrow free) \begin{cases} 0, & C_2 > C_1 \\ \dfrac{f(C_2) - f(C_1)}{1 - f(C_1)}, & C_2 < C_1 \end{cases} \tag{3}$$

Similar to Nordam et al. (2019a), Arneborg et al. (2017) also considers that particles will move as in an ice-free ocean for $C < 30\%$ and with the ice field for ≥80%.

2.3. Drifter trajectories

The simulated spill trajectories were compared to observed drift of buoys from the International Arctic Buoy Program (IABP) in the period between November and April (2018/2019, 2019/2020). 140 *Level 1* trajectories were downloaded from the IABP server (https://iabp.apl.uw.edu/WebData/) and these were evaluated under quality control tests (impossible date, impossible location, duplicated dates and spike removal) and data processing measures (resampling and linear interpolation). 52 tracks were disregarded after these first two steps due to the presence of various spikes in sequence and/or jumps in the time series. The remaining 88 trajectories were then evaluated against sea ice concentration observations from the European Organisation for the Exploitation of Meteorological Satellites (EUMETSAT) Ocean and Sea Ice Satellite Application Facility (OSI-SAF, National Snow and Ice Data Center (NSIDC), 2017) product in order to ensure that their displacement occurred in sea ice conditions. The OSI-SAF daily product has a horizontal resolution of 10 km and it was spatially interpolated to the observed trajectories over the first 15 days of drift. Finally, 55 trajectories with 1 h sampling period were considered reliable. Fig. 1 shows the drifter trajectories before (*a*, 140 beacons) and after (*b*, 88 beacons) the quality control and data processing procedures, with their initial position represented by red dots. In *b*, the 33 red trajectories are neglected in this work because they are in ice-free water. We focus on the 55 black trajectories drifting in sea ice areas.

The second set of observations is composed by four trajectories of wave sensors (14432, 14435, 14437 and 14438) deployed between 12 and 14 September 2018 on ice floes in the marginal ice zone (MIZ) at around 250 km north of Svalbard during the fourth Nansen Legacy (AeN) research cruise. The icebreaker was steaming perpendicular to the estimated ice edge in the course of the deployment, towards regions of higher ice concentration. As a consequence, the first instrument was deployed on a solitary ice floe in the outer MIZ, while the second was set in dense drift ice, the third at the beginning of closed drift ice and the fourth further inside the pack ice.

Each instrument features a high accuracy Inertial Motion Unit (IMU), in the present case the VN100 from Vectornav (Vectornav Corporation, 2019), which has been used in a number of previous studies (Rabault et al., 2017; Marchenko et al., 2017; Rabault et al., 2016; Sutherland and Rabault, 2016). While the design of the instruments is focused towards measurements of waves in ice, each of them also includes a GPS that provides accurate localization. Finally, an Iridium modem is used to remotely transmit the data. In the following, the tracking feature of the instruments will be exploited. As the instruments were deployed on ice floes, they effectively allow to monitor the Lagrangian ice drift. Transmission of data happens with a period of around 5 h. Since the instruments are equipped with large batteries and solar panels, trajectories should in theory be available for long periods of time. However, in practice, a large storm incoming from the North Atlantic ocean led to loss of contact after around 2 weeks for the instrument that survived the longest. Over the corresponding period of time, the total drift length is about 340 km (Rabault et al., 2020).

Mounted ice floes and buoys deployed at the ocean surface have been extensively used in oil slick tracking and modeling. By tracking mounted ice floes, Faksness et al. (2011) observed that the oil released in the marginal ice zone north of Svalbard (70% ≤ C ≤ 80%) during the JIP field experiment drifted with the ice field (Sørstrøm et al., 2010).

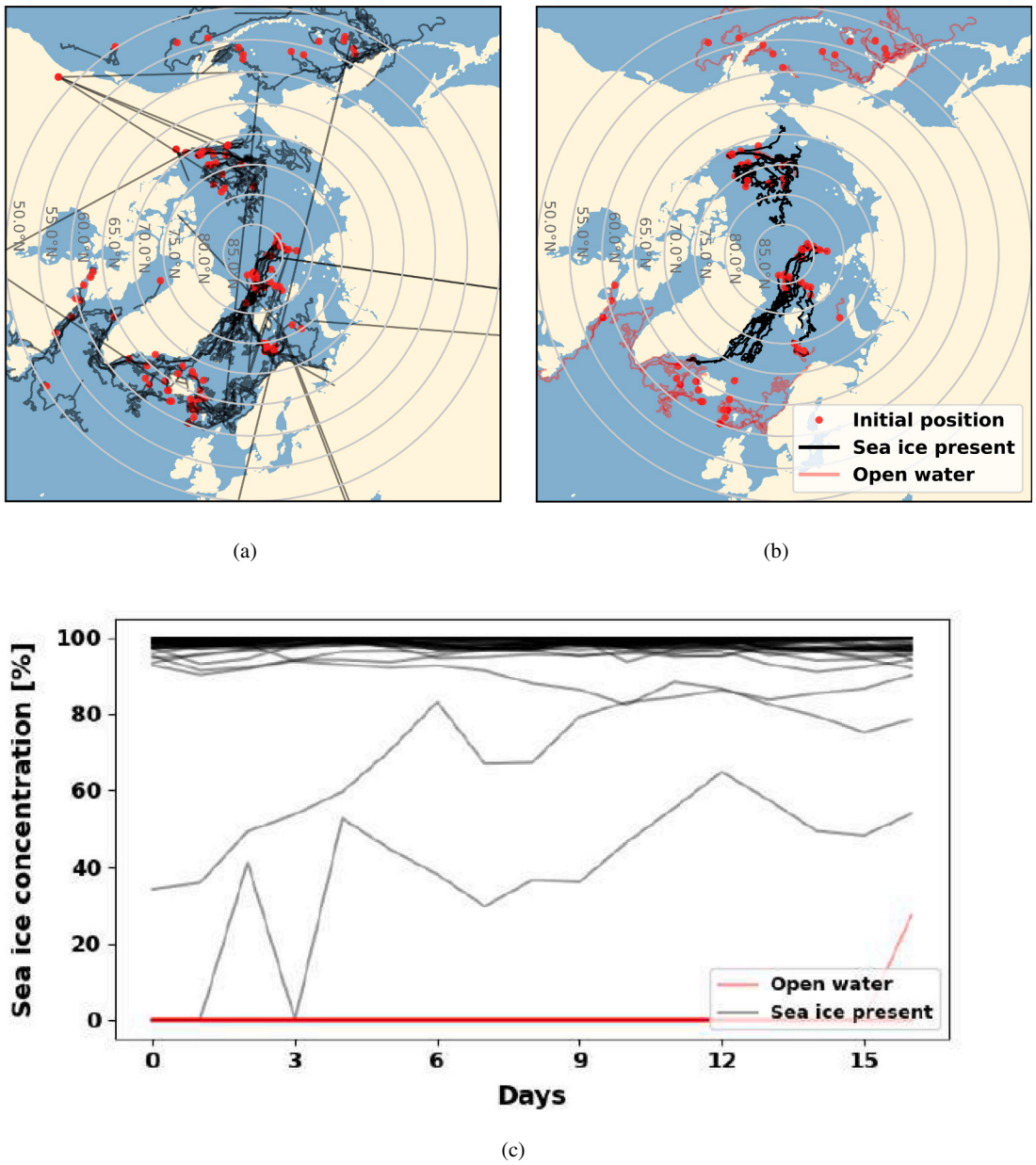

Fig. 1. IABP drifters before (a, 140 trajectories) and after (b, 88 trajectories) data processing and quality control. Red dots represent their deployment position. Panel (c) shows sea ice concentration values from OSI-SAF interpolated to drifters in (b) over their first 16 days. The colors of trajectories in (b) represent the presence (black) or absence (red) of sea ice, as shown by the same colors in (c). (For interpretation of the references to colour in this figure legend, the reader is referred to the web version of this article.)

French-McCay et al. (2018) and Beegle-Krause et al. (2017) used these observations and IABP buoy trajectories to evaluate SIMAP and OSCAR oil-in-ice transport and fate models, respectively. For open waters, good correspondence between buoy and surface oil drifts was found by Price et al. (2006); Jones et al. (2016); Brekke et al. (2021). These studies indicate that such devices can be used to represent oil drift in both sea ice covered and ice-free waters.

2.4. Atmospheric and ocean forcing

As an offline framework, particles in OpenDrift are forced by external metocean model outputs. Due to non-overlapping periods of the considered numerical modeling experiments (see Section 2), different products were used to perform the simulations and these are described below.

Two different ocean-sea ice models were used for the IABP and AeN trajectory simulations, namely the operational version of Towards an Operational Prediction system for the North Atlantic European coastal Zones *v*. 4 (Sakov et al., 2012) (TOPAZ4), and the Canadian Regional Ice and Ocean Prediction System (RIOPS) (Dupont et al., 2015). The first is available at Copernicus Marine Environment Monitoring Service (2018) while the outputs from the latter can be downloaded at http://dd.alpha.weather.gc.ca/yopp/. The atmospheric forcing for these simulations were obtained from the Canadian Arctic Prediction System (Casati et al., 2021), which can also be found in the latter data server.

TOPAZ4 is a coupled ice-ocean data assimilation system for the North Atlantic and the Arctic based on Ensemble Kalman Filter (EnKF) with 100 dynamical members (Sakov et al., 2012). The EnKF is used to assimilate data of both satellite and *in situ* measurements in near real time and from reanalysis products. Its hydrodynamic model (HYCOM *v*. 2.2.18) is coupled with the Los Alamos Sea Ice Model (CICE) and with an ecosystem model, the ECOSMO (Schrum et al., 2006). Covering the

whole Arctic with a resolution between 12.5 and 16 km (1/8°), TOPAZ4 was developed and is maintained by the Nansen Environmental and Remote Sensing Center (NERSC) and runs operationally for the Arctic – Monitoring Forecasting Centre of the Copernicus Marine Environment Monitoring Service (CMEMS ARC-MFC) at the Norwegian Meteorological Institute (Simonsen et al., 2019). Inheriting CICE's functionalities, TOPAZ4 presents an elastic-viscous-plastic (EVP) sea ice rheology (Hunke and Dukowicz, 1997). Hereinafter, this hourly product will be referred as *TOPAZ4-H*.

Developed and maintained by the Environment and Climate Change Canada (ECCC) as a contribution to the Year of Polar Prediction (YOPP), RIOPS provides 48 h ice and ocean forecasts four times a day for the region situated between the Bering Strait to 26°N in the North Atlantic Ocean. With a spatial resolution between 3 and 8 km (1/12°) and hourly averaged surface fields, RIOPS ice-ocean initial conditions are downscaled from the Global Ice and Ocean Prediction System (GIOPS, Smith et al., 2016). The RIOPS ocean model engine is the Nucleus for European Modelling of the Ocean (NEMO *v*. 3.6) and the sea ice model is CICE 4.0, with the same sea ice rheology as TOPAZ4 (EVP). In fact, RIOPS is an extension of the Regional Ice Prediction System (Lemieux et al., 2015) and as such, RIOPS also counts with data assimilation of sea ice concentration from passive microwave satellites.

RIOPS is coupled with the Canadian Arctic Prediction System (CAPS) and the latter provides the atmospheric forcing to the ice-ocean model. CAPS is downscaled from the Global Deterministic Prediction System (GDPS), also developed and maintained by ECCC, and presents a spatial grid resolution of 3 km covering the whole Arctic. TOPAZ4-H, on the other hand, is forced at the sea surface by the European Centre for Medium-Range Weather Forecasts (ECMWF) operational analysis. With a horizontal resolution of 0.1° x 0.1°, ECMWF provides atmospheric fields such as dew point temperature, sea level pressure, air temperature at 2 m height and wind speed at 10 m height to TOPAZ4.

In order to reproduce the hypothetical oil spill (see second numerical modeling experiment), different inputs were used; namely the TOPAZ4 reanalysis (hereinafter *TOPAZ4-R*), the Nordic Seas 4 km numerical ocean model hindcast archive (SVIM, Lien et al., 2013) and the NORA3 product as atmospheric and wave forcing (Haakenstad et al., 2021). The first extends from 1991 to 2018. With daily mean outputs, it is initialized in 1979 with the World Ocean Atlas climatology and it is forced at the ocean surface by the 5° ECMWF ReAnalysis (ERA5). TOPAZ4-R also counts with a data assimilation system and its horizontal resolution and sea ice rheology are the same as the operational version (TOPAZ4-H) (Xie and Bertino, 2021). The data set is freely available at Copernicus Marine Environment Monitoring Service (2018) as well.

SVIM is a 4 km horizontal resolution hindcast that covers the period between 1960 and 2018 (Lien et al., 2013). The model domain extends from the Nordic Seas to parts of the Arctic Ocean, including the Barents Sea, Pechora Sea and the Kara Sea and provides daily outputs. The model core is based in the Regional Ocean Modeling System (ROMS), with 32 vertical sigma levels and is forced at the ocean surface by the NOrwegian ReAnalysis 10 km (NORA10). Oceanic initial and boundary values were derived from the Simple Ocean Data Assimilation data set version 2.1.6 (SODA 2.1.6), whereas for sea ice, they were obtained from MICOM (Miami Isopycnic Coordinate Ocean Model). The ice dynamics is also based on the EVP rheology and the tidal forcing on TPXO4.

The last product considered is NORA3 (Haakenstad et al., 2021; Solbrekke et al., 2021), a new atmospheric hindcast that covers the Norwegian Sea, the North Sea, the Barents Sea and part of the Arctic Ocean. NORA3 is an ERA5 dynamically downscaled product obtained by using the 3 km horizontal resolution, nonhydrostatic numerical weather prediction model HARMONIE-AROME. The hindcast outperformed NORA10 and ERA5 in the reproduction of maximum wind speed observed in 12 out of 19 polar low centers and in the representation of near-surface winds over open ocean and coastal terrains (Haakenstad et al., 2021).

As described below, the set of numerical modeling experiments considered in this work cover different periods and locations. Higher resolution ocean-ice models, although extremely valuable, are often limited in area coverage (*Barents-2.5 km*) or do not present a sufficiently long output record (*e.g.* neXtSIM, Rampal et al., 2016), making them impractical for use here. The previously described products are freely available and can be quickly accessed to support real case operations regarding the user jurisdiction or affiliation.

2.5. Experimental design

Two sets of numerical modeling experiments were defined for the evaluation of the two oil-in-ice drift models. The first one intended to reproduce the IABP and AeN drifter trajectories. For these simulations, 1000 virtual particles were released at the initial position of every drifter and forced for 15 days by CAPS and ice-ocean inputs from TOPAZ4-H and RIOPS. For this same data set, the simulations were re-initialized every three days and forced for this same number of days. For the AeN drifters, simulations had to be shortened due to their shorter life span (between 7 and 12 days). CAPS, TOPAZ4-H and RIOPS were also used in this set of simulations.

The observed and simulated trajectories were compared using the normalized cumulative Lagrangian separation proposed by (Liu and Weisberg, 2011) (*Liu skill* hereinafter). This metric is based on the ratio between the normalized cumulative separation distance (d) and the cumulative length of the observed trajectory (dl):

$$s = \frac{\sum_{i=1}^{N} d_i}{\sum_{i=1}^{N} dl_i} \tag{4}$$

where d_i is the separation distance between the modeled and the observed points of the trajectories at time step i after the model initialization ($i = 0$), dl_i is the cumulative length of the observed trajectory and N is the total number of positions.

The Liu skill is defined as:

$$ss = \begin{cases} 1 - \frac{s}{n}, & \text{if } s \le n \\ 0, & \text{if } s > n \end{cases}, \text{where } n \text{ is a tolerance threshold.} \tag{5}$$

The tolerance threshold $n = 3$ was considered. Although the choice of such threshold is arbitrary, it defines the expectations or requirements to the model (Liu et al., 2014). The perfect fit between modeled and observed trajectories occurs when the distance d_i is zero ($s = 0$) and hence $ss = 1$.

The second numerical modeling experiment simulated a hypothetical oil spill accident in the Pechora Sea (71°N, 49°E) located in the southern Barents Sea and next to the Kara Gate. Backtrack studies (*e.g.* Huserbråten et al., 2019) have supported evidences that Polar cod (*Boreogadus saida*) spawning areas in the Barents Sea seem to be split in at least two different regions, with the most important of them being located in the vicinity of Kara Gate, where the releasing point was placed. The conceptualization of this numerical modeling experiment is based on similar simulations conducted by Röhrs et al. (2018); Morell Villalonga et al. (2020).

A set of stochastic simulations (300 simulations × 2 oil-in-ice drift models x 2 ice-ocean products) were performed by randomly initializing the models at different start dates between March and May (1998–2017), with coefficients (windage factor and horizontal diffusion) varying for each run. 100 particles were released in each of the 2D oil spill simulations and they were forced for 10 days by SVIM and TOPAZ4-R ice-ocean fields, with wind inputs from the NORA3 hindcast. The trajectories were inter-compared using the skill score proposed by Willmott (1981), which is given by:

$$d = 1 - \frac{\sum_{i=1}^{N} \left(A^i - N^i\right)^2}{\sum_{i=1}^{N} \left[\left|A_i^*\right| + \left|N_i^*\right|\right]^2} \quad (6)$$

where A is the position time series (latitude or longitude) under Arneborg et al., 2017 approach, N is the corresponding time series under Nordam et al., 2019a model. $A^* = (A - \overline{N})$ and $N^* = (N - \overline{N})$, where $\overline{N}$ is the time series mean. This skill score ranges between 0 and 1, where 1 represents the perfect agreement between the two series and 0 expresses total discordance. The surface area covered by the cloud of particles at the last time step was estimated using the concave hull algorithm based on Delaunay triangulation and the distance traveled by the particles from the releasing point was compared to the sea ice concentration values of the corresponding forcing. The flow chart representing the work structure is presented in Fig. 2.

It is well known that entrainment and the oil type, hence the weathering properties, do affect the surface oil drift (Röhrs et al., 2018), but these were neglected in order to simplify the analysis and avoid external interference that might affect the modeled trajectories. The same oil (Marine Diesel, ESSO), $\rho = 852.06$ kg m^{-3} and $\mu = 0.006$ kg m^{-1} s^{-1}, was used in all simulations.

3. Results

3.1. IABP simulations

The first numerical modeling experiment intended to simulate the trajectories of IABP and AeN drifters deployed in the Arctic. Regarding the first, 15-days period simulations were conducted and the separation distance between observed and modeled trajectories for the 4 combinations between the oil-in-ice (Arneborg et al. (2017); Nordam et al., 2019a) and the coupled ice-ocean models (RIOPS and TOPAZ4-H) are presented in Fig. 3. The mean separation distance (μ, black thick line) and the standard deviation (σ, grey shaded area) are also shown. The vertical, red dashed lines indicate every third day of simulation (3, 6, 9, 12 and 15) and their correspondent mean separation distance values are

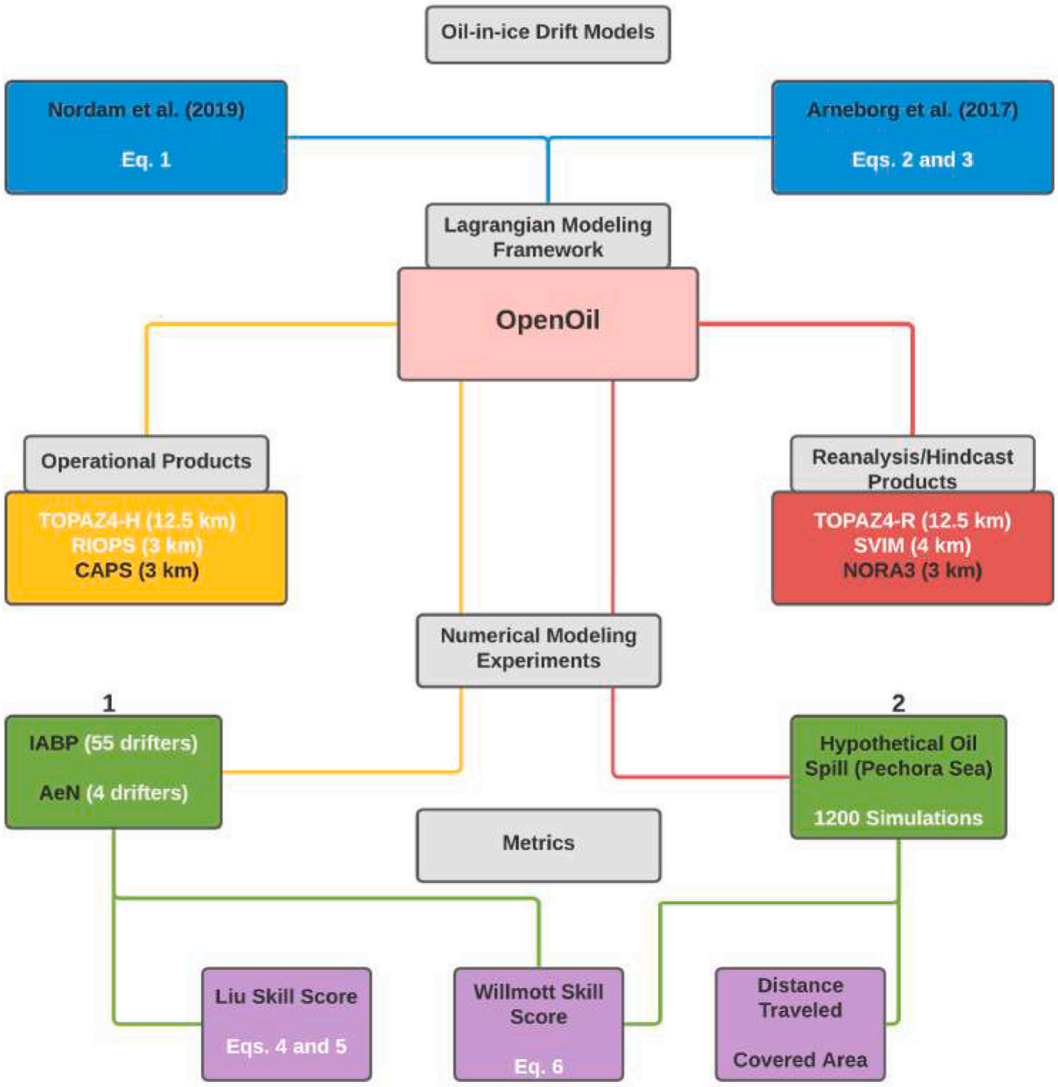

Fig. 2. Flow chart representing the work design. Upper blocks: the two oil-in-ice drift models coded in the Lagrangian modeling framework (middle block, OpenOil). Operational (yellow block) and hindcast/reanalysis (red block) atmospheric (white text) and ice-ocean products are used as forcing in the different numerical modeling experiments (green boxes). The first numerical modeling experiment (left, 1) simulates the oil trajectory in the ice pack (IABP, 55 drifters) and in the MIZ (AeN, 4 drifters) and the second one (right, 2) a hypothetical oil spill in the Pechora Sea (March–May 1200 simulations). The outputs are then evaluated using different metrics, shown in the purple boxes. See the text for further information. (For interpretation of the references to colour in this figure legend, the reader is referred to the web version of this article.)

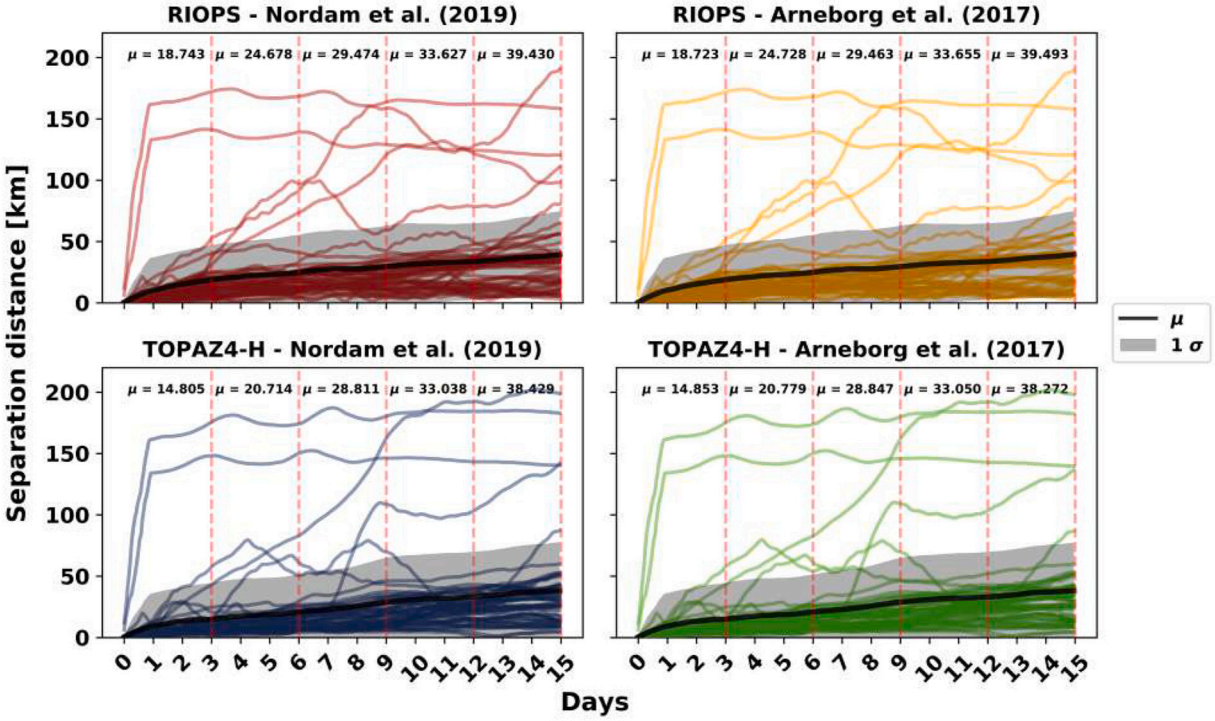

Fig. 3. Separation distance [km] for the 15-day period runs of IABP buoys simulated by the two oil-in-ice drift models (Nordam et al. (2019a) - left column; Arneborg et al. (2017)- right column) and forced by RIOPS (top row) and TOPAZ4-H (bottom row). The mean separation distance (μ) is represented by the thick black line and the standard deviation (σ) by the shaded area. Vertical, dashed lines are plotted every three days and their corresponding μ, in km, is presented on the left side.

exhibited too.

By visual inspection of Fig. 3, one can observe that the four combinations presented similar separation distances, especially when comparing the different oil-in-ice drift models forced by the same ice-ocean inputs. Around 90% of the values are located within the 1σ envelope. Similarly, all of the four set of simulations were unable to satisfactorily reproduce the same drifters. The mean separation distances of both oil-in-ice drift models forced by TOPAZ4-H (38.428 km

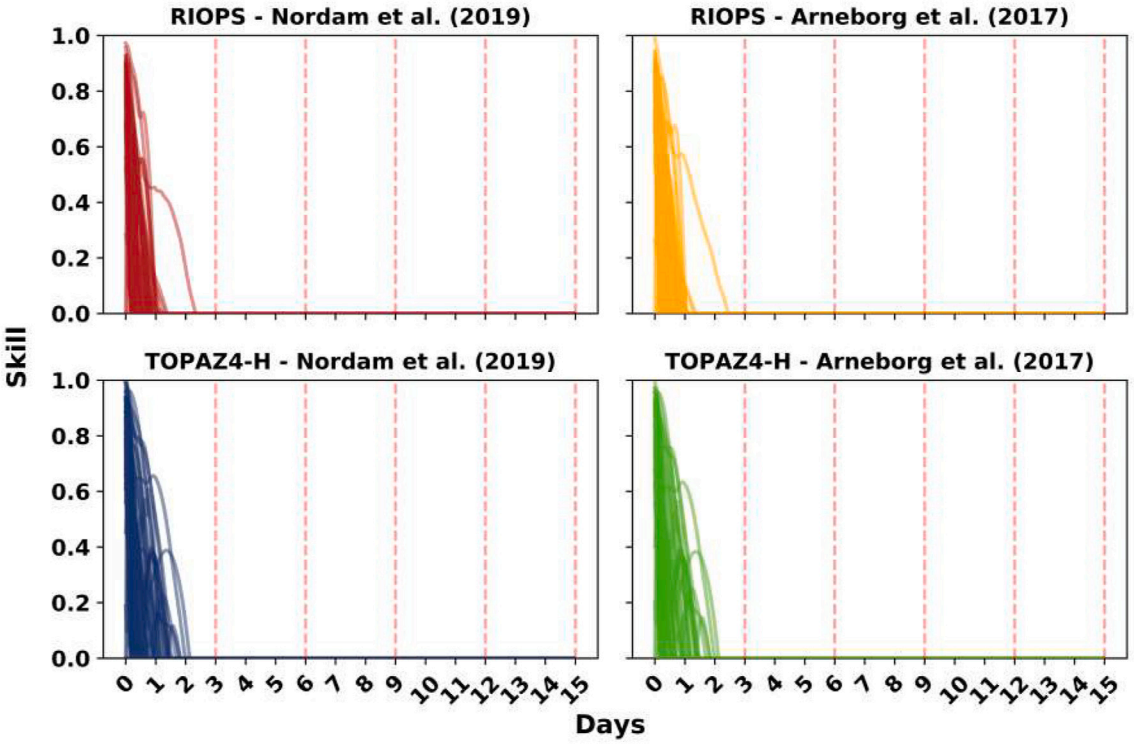

Fig. 4. *Liu skill* values for the 15-day period runs of IABP buoys simulated by the two oil-in-ice drift models (Nordam et al. (2019a) - left column; Arneborg et al. (2017) - right column) and forced by RIOPS (top row) and TOPAZ4-H (bottom row). Vertical, dashed lines are plotted every three days.

and 38.272 km) are smaller than when simulations were performed with RIOPS (39.430 km, 39.493 km), although the rate of growth of the latter is slightly smaller, 1.6 km day^{-1} and 1.4 km day^{-1}, respectively. On the 15th day of simulation, the model proposed by Arenborg et al. (2017) and forced by TOPAZ4-H presented the lowest mean separation distance (38.272 km), about 1.2 km less than the the worst combination, Nordam et al., 2019a forced by RIOPS (39.430 km).

The skills for this set of simulations, calculated using Eq. (5), are

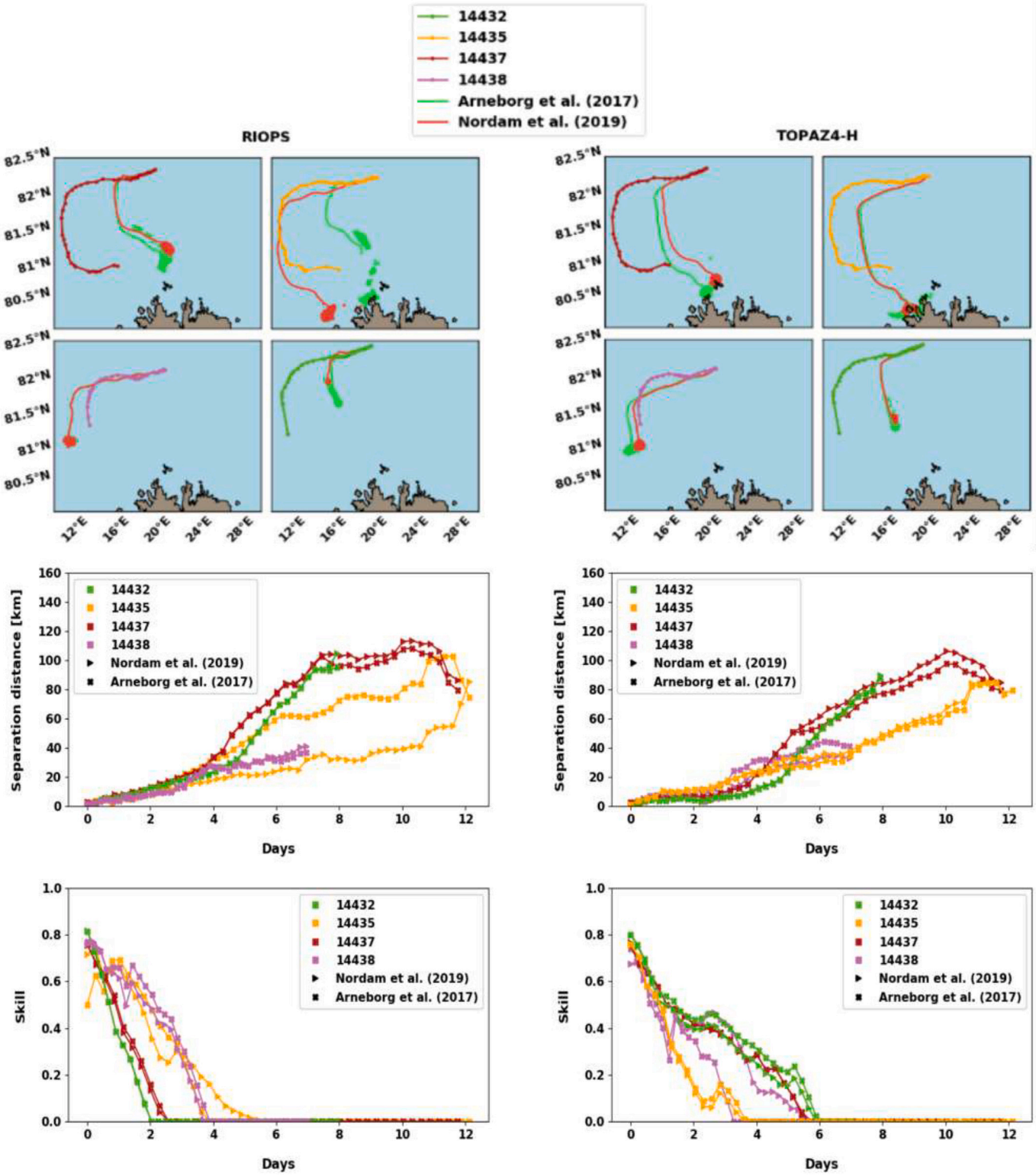

Fig. 5. Simulated (solid lines) and observed (with markers) trajectories (top row), separation distance [km] (mid row) and skill values (bottom row) for the AeN drifters forced by RIOPS (left column) and TOPAZ4-H (right column). Nordam et al. (2019a) (Arneborg et al. (2017)) oil-in-ice drift approach is represented by the light red (green) solid line in the trajectory maps and by the square (triangle) markers in the second and third row. Solid colors represent each of the four drifters, as indicated in the legend. (For interpretation of the references to colour in this figure legend, the reader is referred to the web version of this article.)

presented in Fig. 4. One can notice that the values decay fast, reaching no skill at around 1 day after the initialization for simulations forced by RIOPS and after about 2 days under TOPAZ4-H forcing. Similar to the separation distances, there is essentially no difference between different oil-in-ice drift models when forced by the same ice-ocean product.

3.2. AeN simulations

Regarding the four drifters deployed during the AeN cruise, Fig. 5 shows the modeled trajectories (first row), the separation distances (km, second row) and the Liu skill (third row) for simulations forced with RIOPS (left column) and TOPAZ4-H (right column).

The trajectory maps (Fig. 5, top row) indicate that the observed drifts (colored, marked lines) are generally poorly represented by the drift models (Nordam et al. (2019a) - pink; Arneborg et al. (2017) - lime green). Apart from beacon 14438 and 14435 forced by RIOPS under Nordam et al. (2019a) approach, particles seem to have drifted westward less than the observed trajectories although their shape are somehow similar. One can also notice that the eastward shift in the longer drifts (14435 and 14437) was not satisfactorily represented by the models. Moreover, with the exception of beacon 14438, the cloud of particles under Arneborg et al. (2017) approach presented an apparently higher extent of dispersion whereas particles ruled by Nordam et al. (2019a) model drifted more cohesively, highlighting the difference between the two oil-in-ice drift models.

The separation distances seem to increase almost linearly in the first four days, reaching around 18 km on the third day. After that, the values corresponding to beacons 14437 and 14432 sharpened their trend and increased from 30 km to about 100 km in four days (4th to 8th day). Notwithstanding this change, the separation distances related to beacon 14435 grew apparently at constant rate throughout the simulation.

The Liu skill values (bottom row, Fig. 5) suggest slightly better results towards simulations forced by TOPAZ4-H. Regarding the latter, from the eight simulations, five of them presented skill values higher than 0 beyond the 4th day of simulation, whereas only one (beacon 14435, under Nordam et al. (2019a) approach) extended for more than four days with $SS > 0$ in the runs forced by RIOPS. The skill characteristics relative to each buoy are not the same for RIOPS and TOPAZ4-H. For example, while skill values associated with beacons 14432 (green) and 14437 (red) have the sharpest decay under the first forcing, reaching the no-skill level before 3 days, the same beacons last the longest when TOPAZ4-H was used.

3.3. Hypothetical oil spill in the Pechora Sea

1200 simulations were performed for the hypothetical oil spill in the Pechora Sea using TOPAZ4-R and SVIM as ocean inputs and NORA3 as atmospheric forcing. Covering the period between 1998 and 2017 (March–May), 120,000 particles were released and tracked for 10 days. The distribution of particles at the last time step of the simulations is presented in Fig. 6. Similar to the previous results, the choice of the oil-in-ice model seems to be a minor constraint in 2D oil drift modeling in

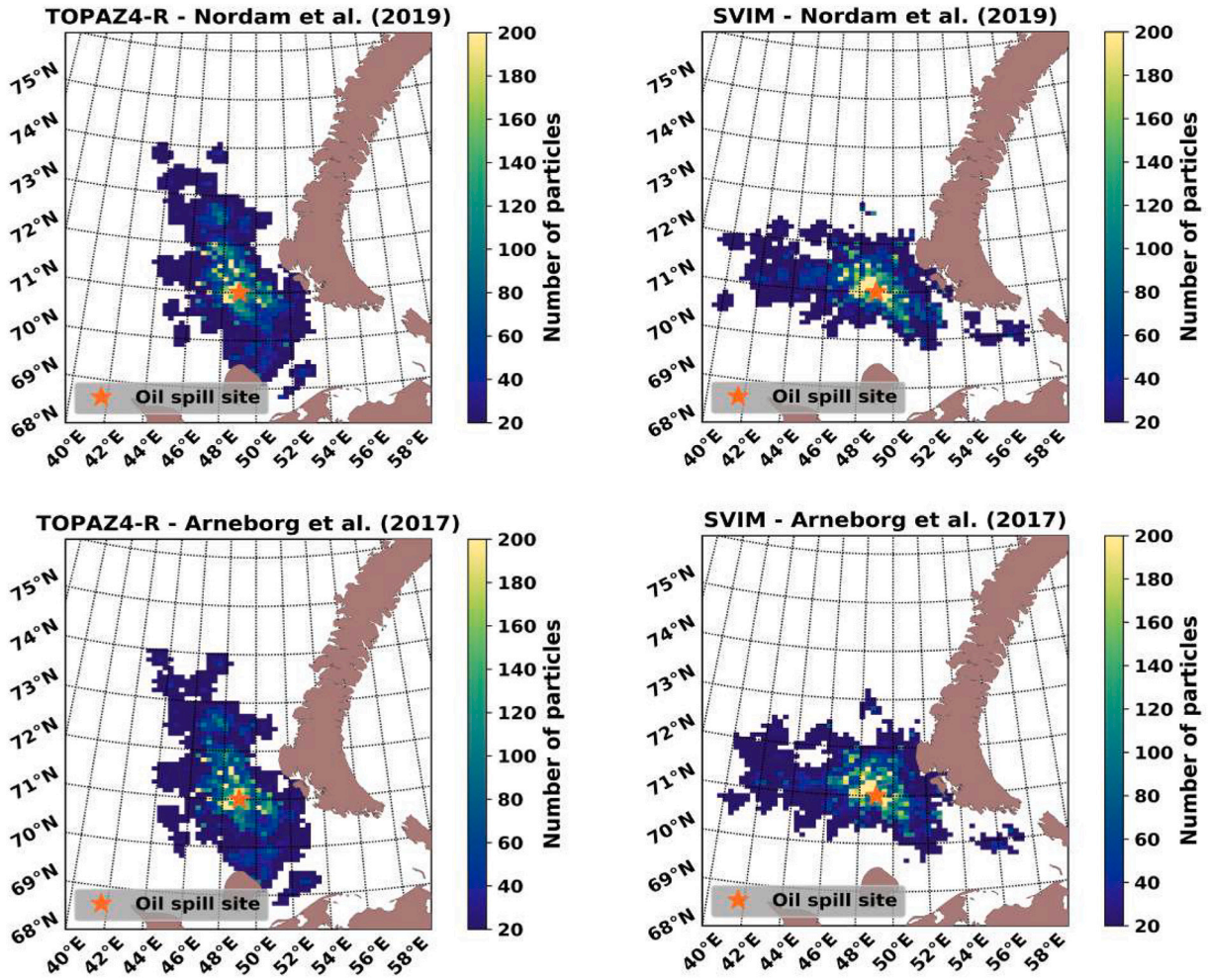

Fig. 6. Horizontal concentration maps (number of particles) at the last time-step for stochastic oil spill simulations after 10 days summed over the 1200 simulations. Forcings are displayed in the columns (TOPAZ4-R - left; SVIM - right) and oil-in-ice models in the rows (Nordam et al. (2019a) - top; Arneborg et al. (2017) - bottom).

the presence of sea ice.

Simulations forced by SVIM presented a larger zonal distribution, extending from 40°E to 57°E, but limited within the meridional band between 70°N and 72°N. Conversely, when forced by TOPAZ4-R, particles covered a greater latitudinal extension, reaching the Kolguyev Island at 69°N and beyond 73°N, but bounded within 44°E and 52°E. The estimated area covered by the particles was larger in TOPAZ4-R simulations (87,076 km^2; 91,687 km^2) than in SVIM (72,873 km^2; 77,893 km^2), for Nordam et al. (2019a); Arneborg et al. (2017), respectively.

Comparing the simulated trajectories, it is shown in Fig. 7 the Willmott skills time series of latitude and longitude calculated with Eq. (6) for the different oil-in-ice drift models (Nordam et al. (2019a) and Arneborg et al. (2017)) and forcings (SVIM and TOPAZ4-R). Simulations realized with different oil-in-ice drift models, but forced with the same model products, resulted in high Willmott skill values (>0.9) and low spread, indicating high similarity between the trajectories. Conversely, marked by a widespread distribution of values, an oil-in-ice model forced by different ice-ocean products clearly produced more variability in the outputs. Similar results were obtained for the other numerical modeling experiments (IABP & AeN, not shown), indicating that such a pattern is consistent regardless the considered sea ice conditions.

Since the spatial distributions of particles forced by the same input are remarkably similar (Fig. 6), only results related to the Nordam et al. (2019a) approach are shown in Fig. 8, with simulations forced by SVIM and TOPAZ4-R on the left and right columns, respectively. The top-row shows the relationship between the yearly-averaged distance traveled (km) by the cloud of particles' barycenter and the associated mean sea ice concentration (%). The colored scatter represents the years of the period of interest (1998–2017) and the adjusted linear regression is depicted by the solid red line. The adjusted linear regression indicated a negative relation between the variables, with a slope (correlation) of −1.28 km/% (−0.85) for SVIM and − 1.20 km/% (−0.85) for TOPAZ4-R. Put in words, decreasing sea ice concentration allow slicks to drift further away from their releasing point.

The mid-row in Fig. 8 exhibits the intra-annual variability of sea ice concentration stored by the virtual particles. The values indicated a shift from high (>90%, 1998 and 1999) to low sea ice concentration (<30%, 2011–2017) in SVIM (Fig. 8). The large inter-quartile range between these two periods (2000−2010) might represent the transition of the sea ice concentration field, marked by high variability. This is not however observed in the simulations forced by TOPAZ4-R, in which low values were consistently present since 2001.

As mentioned previously, the distance traveled by the particles and the sea ice concentration are statistically related and since the latter was generally lower in the TOPAZ4-R simulations, one could also expect that oil slicks would drift further away from the releasing point when forced by this ice-ocean inputs. In alignment with these findings, Fig. 8 (bottom row) exhibits the intra-annual variability of distance traveled by particles over the considered period and the results revealed that particles traveled about 12% more under TOPAZ4-R forcing. Despite the difference in magnitude, the interannual variability is similar between the two outputs (SVIM *vs* TOPAZ4-R), suggesting that the wind forcing might be the common factor modulating the drifts.

4. Discussion

In this study, two oil-in-ice drift models proposed by Nordam et al. (2019a) and Arneborg et al., (2017) were implemented in OpenDrift (Dagestad et al., 2018), an open-source Lagrangian framework developed and maintained by the Norwegian Meteorological Institute, and assessed through two sets of simulations: (I) the reproduction of drifter trajectories in the ice pack (IABP) and in the marginal ice zone (AeN), and (II) a hypothetical oil spill in the Pechora Sea.

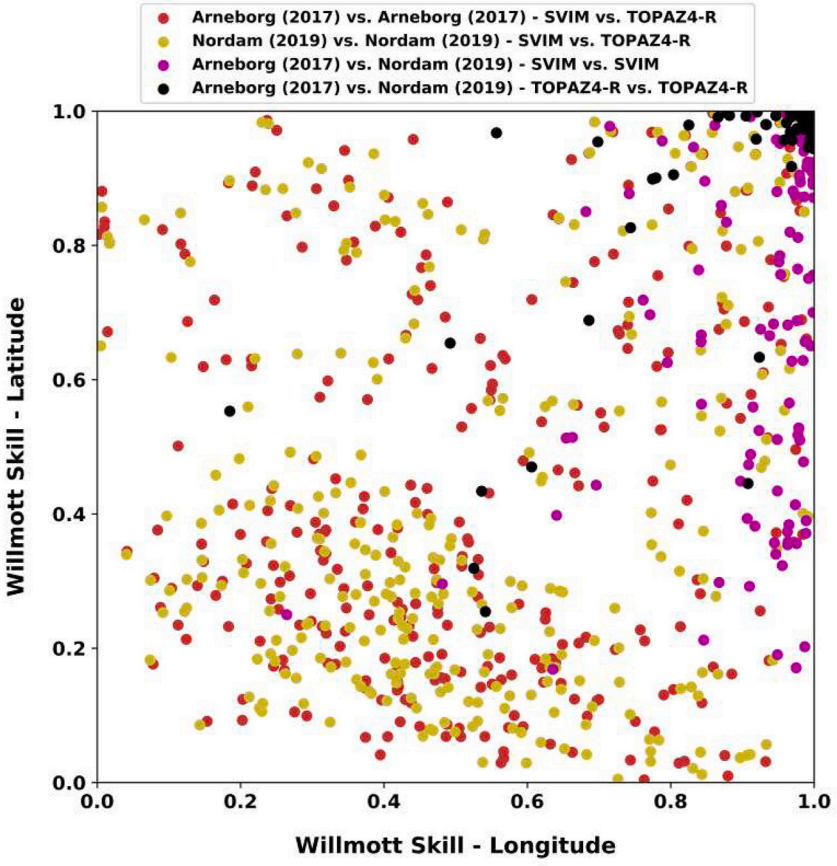

Fig. 7. Inter-compared Willmott skill values (Eq. (6)) for simulated trajectories from the hypothetical oil spill (disentangled into longitude - horizontal axis and latitude - vertical axis). Each colour represents a combination between oil-in-ice models (Nordam et al. (2019a) and Arneborg et al. (2017)) and forcings (TOPAZ4-R and SVIM): red – Arneborg et al. (2017) *vs.* Arneborg et al. (2017) forced by SVIM and TOPAZ4-R; yellow – Nordam et al. (2019a) *vs.* Nordam et al. (2019a) forced by SVIM and TOPAZ4-R; purple - Arneborg et al. (2017) *vs.* Nordam et al. (2019a) forced by SVIM; black - Arneborg et al. (2017) *vs.* Nordam et al. (2019a) forced by TOPAZ4-R; (For interpretation of the references to colour in this figure legend, the reader is referred to the web version of this article.)

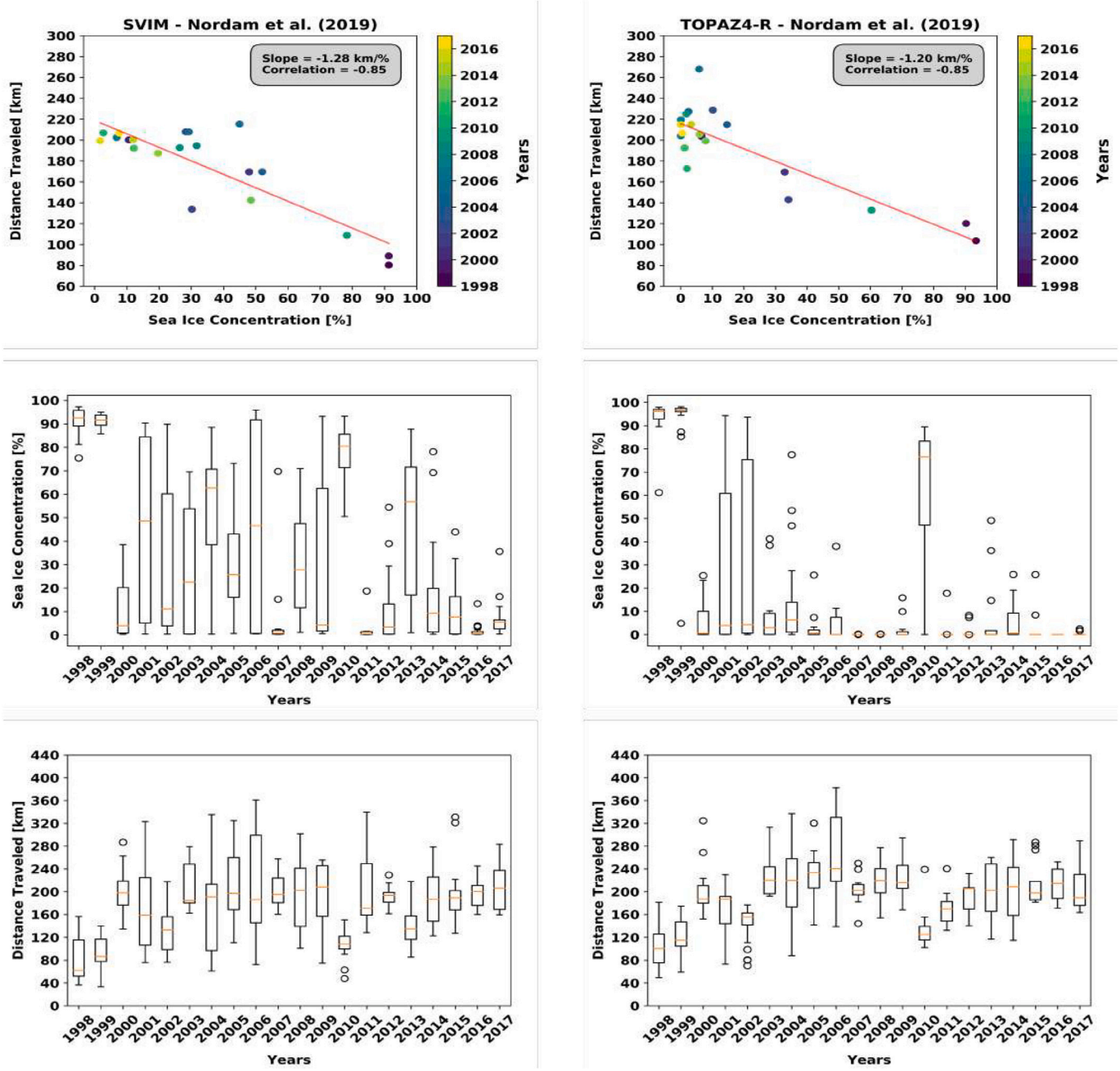

Fig. 8. Correlation between yearly averaged sea ice concentration [%] and distance traveled [km] by the cloud of particles from the releasing point (top row), yearly distribution of sea ice concentration [%] (mid row) and distance traveled [%] for the 300 simulations under Nordam et al. (2019a) oil-in-ice approach forced by SVIM (left column) and TOPAZ4-R (right column). The orange line in the boxplots represent the median. The red line in the top row plots represents the fitted trend line adjusted by linear regression and the colorbar represents the studied period, 1998 (blueish) - 2017 (yellowish). (For interpretation of the references to colour in this figure legend, the reader is referred to the web version of this article.)

4.1. Trajectories in the ice pack - IABP

For the simulations performed in the ice pack (IABP drifters) (Fig. 3 and Fig. 4), TOPAZ4-H provided slightly better results than RIOPS in terms of mean separation distance and skill values, but the oil-in-ice drift models responded essentially equal under a same forcing. The latter outcome was somehow expected since the main difference between the two oil-in-ice drift models materialize in transition zone $30\% < C < 80\%$. Nonetheless, the results obtained for the simulations conducted in the marginal ice zone north of Svalbard (AeN) also indicated that the choice of the oil-in-ice drift approach might be less relevant for 2D simulations than the considered forcing.

It is not obvious why the higher resolution model (RIOPS) did not present better results than TOPAZ4-H. These results coincide with the observations made by de Vos et al. (2021) that increasing grid resolution is not a guarantee of a better performance if sea ice parameterizations are not improved. Similar results were found for drifters deployed in the North Sea and Norwegian Sea, where the lack of improvement was related to the ill description of mesoscale features by the non-assimilative high resolution (≈2.4 km horizontal resolution) regional model NorShelf (Dagestad and Röhrs, 2019).

In general, three forces dominate the momentum equation of sea ice, namely the atmospheric and water stress and the internal forces in the ice (Tsamados et al., 2014). The latter relates the stress caused by sea ice

interactions with the deformation of the ice cover (strain) and it is still considered one of the points that limit the performance of ice models despite the variety of approaches Feltham (2008). In this sense, one potential source of the lack of skill improvement in the ice pack is the EVP sea ice rheology scheme, used by the model products considered in this study.

The EVP rheology is currently the most commonly used scheme in operational and global climate models that include sea ice, especially due to its computational efficiency and relatively accurate description of the main, large scale (>100 km) sea ice drift features (*e.g.* Beaufort gyre) (Dansereau et al., 2016). On the other hand, it seems to not satisfactorily reproduce properties at fine scales (Dansereau et al., 2016), which are the most relevant for oil drift operations. By reproducing IABP drifter trajectories using the free drift model and neXtSIM, a dynamic-thermodynamic sea ice model based on Elasto-Brittle (EB) rheology, Rabatel et al. (2018) highlighted how not considering the sea ice strength and interactions (free drift) can rapidly degrade forecasting skills in winter, when the ice pack is more compact. The authors found ensemble mean position errors of 7.5 km for 3-day drift simulations in winter.

French-McCay et al. (2018) also used IABP buoys to validate oil-in-ice drift simulations and their findings indicate improvements in the skill with the EB rheology. French-McCay et al. (2018) found mean separation distances of about 21 km, 35 km and 45 km on the 5th, 10th and 15th day of simulation for ice-ocean models using the EVP whereas it was found in this work d values of about 22 km, 29 km and 39 km for the same correspondent days of simulation. According to the authors, the separation distance decreased to 14 km, 21 km and 26 km when neXtSIM was used.

Although such evidences suggest that the used rheology scheme might be a limiting factor in modeling oil drift in the presence of sea ice, the wind forcing seems to be the primary source of uncertainty even in the ice pack (Cheng et al., 2020). The atmosphere-ice and ice-ocean stresses are proportional to drag coefficients and consequently the accuracy of the ice velocity models greatly depends on how drag coefficients are parameterized (Chikhar et al., 2019). These are strongly related to the boundary layer stability, enhanced (reduced) in unstable (stable) conditions, but the sea ice roughness and its topography might also be considered in the form of frictional skin and form drag components, respectively (Tsamados et al., 2014; Lüpkes and Gryanik, 2015; Martin et al., 2016; Petty et al., 2017). None of the ice-ocean models used here adopts the ice topography dependent form drag coefficient, considered to be more physically realistic (Chikhar et al., 2019).

4.2. Trajectories in the MIZ - AeN

RIOPS seems to have provided slightly better simulations than TOPAZ4-H with respect to the separation distance only for beacons 14,438 and 14,435 using Nordam et al. (2019a) model (second row, Fig. 5). Apart from that and similar to the IABP case, RIOPS did not provide better results in the MIZ either.

Due to its proximity to open waters, drifters in the MIZ can be highly influenced by oceanographic processes considered of minor importance in the ice pack. Johannessen et al. (1992) investigated the ambient noise obtained in a series of acoustic experiments conducted in the Fram Strait, East Greenland Sea and Barents Sea marginal ice zones and their findings indicated high correlation between ice motion and tidal currents. Moreover, the tidal model used by these same authors explained more than 63% of the observed ambient noise. Modeling (*e.g.* Gjevik et al. (1994)) and field observation studies (Seasonal Ice Zone Experiment, 1989 - SIZEX 89) indicated tidal currents with velocities up to 0.8 m s^{-1}, higher than the observed velocity of drifters released in the East Greenland Current during the same experiment (0.3 m s^{-1}). Although tidal currents seem to be an important feature to be taken into account when modeling sea ice drift in the MIZ, and they are in fact considered in RIOPS but not in TOPAZ4-H, such an improvement did not produce better results either.

Beyond tidal variability, ice floes in the marginal ice zone might also be influenced by surface gravity waves. When traveling from the open ocean towards the MIZ, short surface gravity waves are damped by the sea ice and part of the their energy accelerates the floes through wave radiation stress convergence. Numerical studies revealed that such interactions might generate along-edge ice jets (Dai et al., 2019), similar to the ones generated by along-edge jet winds (Heorton et al., 2014). The latter pointed out that such formations can be reliably modeled in model grids with horizontal resolution of 2 km or finer. Feltham (2005) was also able to reproduce an along-edge ice jet by considering the MIZ as a granular media, pointing out that its formation arises naturally as a consequence of the granular nature of sea ice. Muench and Schumacher (1985) observed along-edge jets at speeds of 10–15 cm s^{-1} in the Bering Sea, well above of the 2–5 cm s^{-1} current speeds that typify the region under regular conditions. These submesoscale features have widths of 10–15 km (Johannessen et al., 1983) and can increase the transport of sea ice by 40% in comparison to the ice pack (Heorton et al., 2014). None of the ice-ocean models used here solve wave-ice interactions, present horizontal resolutions of at least 2 km (Heorton et al., 2014) nor treats sea ice as granular material (Feltham, 2005), thus being unable to reproduce this apparently important component of sea ice drift. In addition, the transition of the wind stress over the ice-ocean boundary in the MIZ might create ocean currents parallel to the ice edge associated to upwelling formation (Johannessen et al., 1983).

The aforementioned along-edge currents and jets might be unstable and trigger eddies formation with scales of 10 to 40 km (Johannessen et al., 1983, 1987). RIOPS, and in a lesser extent TOPAZ4-H, are theoretically able to reproduce eddies of this extent, but their eddy-permitting characteristic breaks down when the feature scales approach the internal Rossby radius, $\mathscr{O}$(R), which can be as small as 1–2 km in the Arctic (Sakov et al., 2012). Eddies in the Arctic MIZ, and their role on reshaping the ice edge through basal melting, have been reported since the early 80's (Johannessen et al., 1987), but just recently their characteristics have been assessed by observations (Kozlov et al., 2019) and numerical experiments (Wekerle et al., 2020; Platov and Golubeva, 2020). Despite the different approaches and regions of study, their findings converge to the points that 1) cyclonic eddies are more common than anti-cyclones and 2) their mean radius is about 5 km. In addition, by conducting numerical experiments, Wang et al. (2020) suggested that grid sizes of *at most* 1 km are required to resolve eddies in the Artic basin.

It seems thus reasonable to assume that one of the sources of inaccuracies in this work is the inability of both RIOPS and TOPAZ4-H to accurately resolve the aforementioned processes, generally resulting in poor reproduction of the AeN trajectories.

4.3. The tolerance threshold "n"

The obtained skills for the IABP simulations degraded to 0 (no skill) between 1 and 2 days, faster than reported by French-McCay et al. (2018) that found $SS > 0$ up to 5 days. Unfortunately, the authors did not present the tolerance threshold (n in Eq. (5)) used in their work, thus limiting a direct comparison. Since the mean separation distances found here are actually smaller than the ones obtained by French-McCay et al. (2018), either the tolerance threshold (n) used by them is greater than 3 or the cumulative observed drift here is smaller. Since both works use data from the same region and program, although in different periods, it is likely that the observed trajectories present similar displacements.

When comparing the separation distances found in ice covered regions to the ones obtained in ice-free areas, values are usually smaller in the first. For instance, a mean separation distance of about 22 km after 6 days of simulation (see Fig. 3), whereas Dagestad and Röhrs (2019) obtained a comparable value after only 2 days for drifters released in the North Sea and Norwegian Sea, and Liu and Weisberg (2011) reports mean separation distances of 73 and 27 km after 2 days of simulation for drifters located in ocean interior and continental shelf in the Gulf of

Mexico, respectively. Nonetheless, the observed displacement of drifters in ice-free areas is larger than when released in the ice pack and hence the larger separation distances are compensated by longer drifts.

In this sense, as one can deduce from Eq. (5) but also pointed out by Liu and Weisberg (2011), short observed displacements can largely increase *s* despite *d* being small, thus rapidly decreasing the skill. Using the same tolerance threshold for the simulations conducted in the ice pack (IABP) and in the marginal ice zone (AeN) seems to be unreasonable, and it might explain why skill values for the latter were superior although one can notice by visual inspection that the simulated trajectories in the latter did not reproduce accurately the observed drifts. It is worth highlighting that extending the period of study (beyond 15 days) would probably not decrease the separation distances since the uncertainties present in both oil and atmospheric-ocean-ice models tend to accumulate in time.

The re-initialization of the simulations (not shown) improved the skills in periods of the 15-day IABP runs in which SS values > 0 were not present. Although the mean separation distances being about two to three times smaller relative to their correspondent days in the longer simulations, the skill decay presented the same pattern throughout the re-initialization runs, not extending further than 2 days in the case of particles under TOPAZ4-H and around 1 day when forced by RIOPS. To ensure trackability of oil slicks in real operations, we recommend model re-initializations no longer than 12 h since the last forecasting.

4.4. The implications of sea ice reduction on oil drift - hypothetical oil spill in the Pechora Sea

The last set of simulations reproduced a hypothetical oil spill in the Pechora Sea, next to the Kara Gate, in a region where the sea ice concentration has been significantly changing over the years (see Fig. 6). By randomly selecting the initial releasing date, 300×4 10-day simulations between March–May (1998–2017) were performed.

Converging to the findings presented previously, the results of this experiment also revealed that the ice-ocean forcing is more relevant for 2D oil-in-ice modeling than the choice of the drift approach. The lower sea ice concentration observed in TOPAZ4-R (Fig. 8, middle row) might explain the greater area extent covered by the particles and their longer displacement when compared to simulations forced by SVIM.

The hydrodynamic conditions in the Pechora Sea are mainly controlled by the inflow of the North Cape Current (NtCC), a branch of the Norwegian Atlantic Current (NAC), and the Norwegian Coastal Current (NCC) through the so-called Barents Sea Opening, located between Norway and the Bear Island (Gammelsrød et al., 2009). Once in the Pechora Sea, NtCC is then renamed to Murmansk Current (MC) whereas the NCC to Murmansk Coastal Current (MCC) (Loeng, 1991). Flowing eastwards at first, the NtCC shifts northwards at around 45°E, running parallel to Novaya Zemlya's coastline (Wassmann et al., 2006).

Oil spill modeling studies in the Pechora Sea are still scarce despite the high traffic of tanker ships through the Kara Gate and the presence of oil exploration facilities, including the Prirazlomnaya Arctic oil terminal (69.266°N, 57.285°E). Nordam et al. (2017) simulated hypothetical spills in the Kara Gate and in the Varandey oil terminal, next to Prirazlomnaya, in the present (2009–2012) and future (2050–2053) conditions. The authors identified that the ice cover is extremely important on oil fate prediction, but no considerations were made regarding oil transport. This observation and the previously described ocean surface currents configuration might be an indication of the predominant role of sea currents over the sea ice drift, culminating in the general meridional displacement of particles under the TOPAZ4-R forcing.

The World Wildlife Fundation - Russia (WWF-Russia), through the Risk Informatics Research Guidance Center, conducted a series of oil spill simulations at the location of the Prirazlomnaya terminal in ice-free conditions and in the presence of sea ice. Their findings indicate that during the ice-free conditions particles are able to reach the Kolguyev Island and cross the Kara Gate, located at around 250 km and 150 km away from the spill location, respectively. Conversely, the presence of sea ice limited the oil trajectories to within a radius between 50 km and 75 km, impacting only the near coastline south of the oil terminal (RGC Risk Informatics, 2012). This highlights that the releasing position is an important factor when modeling oil spills in the Pechora Sea.

The Willmott skill obtained by inter-comparing the simulated trajectories (longitude and latitude, Fig. 7) validates the findings made before regarding the similarity of outputs provided by the two different oil-in-ice approaches when forced by the same ice-ocean input. This figure has clearly shown that the spread of values concentrate around 1, indicating high resemblance between the models, especially when TOPAZ4-R was used (black dots). Conversely, using different forcings (yellow and red) produced higher spread of values, which in turn might be a sign of greater importance of ice-ocean models in the simulations variability. Zhang et al. (2020) used two drift models forced by a series of multi-source data set to reproduce the observed trajectory of drifters in the South China Sea in ice-free conditions. The authors also highlighted the dominant role of the ocean forcing over the chosen drift model on the modeling of trajectories in the region.

Although spill accidents are unpredictable, responders nowadays often count with environment information at near-real time and regional assessments that can support faster countermeasure decisions. Such assessments (*e.g.* Spill Impact Mitigation Assessment, SIMA) are strategy plans created through the synergistic effort between researchers, industry, government authorities and society to determine which recovery method will minimize impacts of spills on shared values, such as ecosystem, local business and cultural heritage. As presented above, our findings fairly agree with previous studies and as such OpenOil seems to arise as a valuable open-source resource in oil spill modeling in cold regions, supporting researchers on the evaluation of its impacts in the marine environment in conjunction with other tools, for example SIMA or end-to-end ecosystem models (*e.g.* Hansen et al., 2019).

5. Conclusions

The assessment of two oil-in-ice surface drift models implemented in OpenDrift, an open-source Lagrangian framework developed in Python, was conducted in this work. Proposed by Arneborg et al. (2017); Nordam et al. (2019a), both models are based on the "30/80" rule-of-thumb which states that oil drifts as in open waters when the sea ice concentration $C < 30\%$ and with the ice field when $C \geq 80\%$. For the intermediate values, each model presents a different transition, as shown in Section 2.

The oil-in-ice drift models were evaluated under two different set of simulations: (I) buoys from the IABP program located in the ice pack (2018–2019) and wave sensors released in the marginal ice zone north of Svalbard during the Arven etter Nansen (AeN) cruise in 2018 and (II) a hypothetical oil spill in the Pechora Sea. Due to the different periods of interest, distinct metocean forcing fields were used. For the first set of simulations, the operational TOPAZ4 (TOPAZ4-H), RIOPS and CAPS products were used as forcing while TOPAZ4 reanalysis (TOPAZ4-R), SVIM and NORA3 hindcasts were employed on the hypothetical oil spill in the Pechora Sea.

The findings obtained by applying the skill metrics proposed by Liu and Weisberg (2011) in the first numerical modeling experiment (I) indicate that the observed trajectories were not better reproduced by the finer resolution input (RIOPS), neither in the ice pack nor in the MIZ. A quantitative evaluation of it is out of the scope of the present research and hence they are limited as speculations. In the ice pack, where the IABP buoys were released, the sea ice internal forces and wind-ice stress play a major role on the ice motion, so sensitivity studies regarding sea ice rheology parameterizations and the inclusion of the ice topography on the form drag might improve our understanding of the uncertainties present in sea ice modeling.

For the AeN case, the proximity to the open ocean and the sharp wind drag coefficient transition result in the formation of features not present

in the ice pack and rarely resolved by ice-ocean models. RIOPS does include tidal motions, but this improvement did not provide better results either. In addition, none of the ice-ocean products solve wave-ice interactions, considered as a key factor in the MIZ. Finally, the horizontal resolution of the ice-ocean models seems to not be fine enough to properly reproduce mesoscale motions such as along-edge ice jets and eddies, natural features present in this region.

The separation distances for the IABP numerical modeling experiment are in agreement with previous studies (*e.g.* French-McCay et al., 2018), with a mean value around 38.5 km on the 15th day of simulation and decreasing to less than one third of this when the simulations were re-initialized every three days (not shown). No skill was found beyond the second (first) day of simulation when TOPAZ4-H (RIOPS) was used, indicating that the model must be re-initialized more frequently, ideally not later than 12 h, in real oil spill operations.

The separation distances in the AeN simulations were higher (about 100 km on the 12th day of simulation) despite their shorter life span. The Liu skill values extended up for 6 days, suggesting better agreements between observed and modeled trajectories. Nonetheless, this apparent better performance might be actually a bias associated to the skill formulation itself, more specifically between the arbitrary choice of the threshold parameter n and the distance traveled by the observed drifters. Since the latter is associated to the sea ice concentration, the threshold parameter should be carefully chosen to accommodate the different ice conditions (*e.g.* ice pack or open water) that drifters might be subject to.

The hypothetical oil spill in the Pechora Sea revealed how ice-ocean inputs, in this case SVIM and TOPAZ4-R, produced distinct features of particle trajectories. The sea ice concentration field seems to dictate the spread, the predominant direction of trajectories and the distance traveled by the cloud of particles. The slope (correlation) of the linear regression adjusted between the sea ice concentration and the distance traveled by oil slicks were for the first time presented here and they are statistically significant for both SVIM, −1.28 km/% (−0.85), and TOPAZ4-R, −1.20 km/% (−0.85). The results obtained by intercomparing the simulated drifts from the hypothetical oil spill using the Willmott skill (Eq. (6)) suggest that the two 2D oil-in-ice models provide similar trajectories when forced by the same ice-ocean input. Converging to the findings obtained by Zhang et al. (2020) for open ocean simulations, the choice of the forcing fields seems to play a greater role in the trajectory modeling than the considered drift model.

Our preliminary findings showed that OpenOil, which is already used for official agencies in operational mode for oil spill response in ice-free waters, can be also considered as a potential tool on risk assessment studies and oil tracking monitoring in ice covered regions. As an example of application, the current Norwegian regulations forbid oil exploration December and June in regions less than 50 km away from the observed marginal ice zone between (Faglig Forum, 2019). The results (Fig. 8) for the hypothetical oil spill in the Pechora Sea indicated that the distance traveled by the particles easily overcome this threshold. Further efforts could investigate if such buffer zone is sufficiently wide for protecting the Barents Sea marginal ice zone from accidental oil releases.

Modeling oil fate and transport in the presence of sea ice adds new difficulties to an already hard task. Changes in oil weathering and new transportation possibilities (*e.g.* encapsulation) emerge, thus being of paramount importance continuous development of the model. Such specific processes might also be seen as limitations of this work and they shall be implemented in OpenOil, but we however believe that the free availability of the drift model may motivate independent improvements by the users, making it a resourceful and disseminated tool. Lastly, the scarceness of available drifter data in the marginal ice zone constrains robust analysis and thus an interesting aspect to look at would be the use of a larger data set for the validation of the results presented here.

Abbreviations

AeN	Arven etter Nansen - The Nansen Legacy project
AROME	Applications of Research to Operations at Mesoscale
CAPS	Canadian Arctic Prediction System
CICE	Los Alamos Sea Ice Model
CMEMS ARC-MFC	Arctic – Monitoring Forecasting Centre of the Copernicus Marine Environment Monitoring Service
DMI	Danish Meteorological Institute
EB	Elasto-Brittle sea ice rheology
ECCC	Environment and Climate Change Canada
ECMWF	European Centre for Medium-Range Weather Forecasts
EnKF	Ensemble Kalman Filter
EUMETSAT	European Organisation for the Exploitation of Meteorological Satellites
EVP	Elastic-Viscous-Plastic sea ice rheology
FEX09	Field EXperiment conducted in the Barents Sea in 2009
GDPS	Global Deterministic Prediction System
GIOPS	Global Ice and Ocean Prediction System
IABP	International Arctic Buoy Program
MC	Murmansk Current
MCC	Murmansk Coastal Current
MET	Norwegian Meteorological Institute
MICOM	Miami Isopycnic Coordinate Ocean Model
MIZ	Marginal Ice Zone
NAC	Norwegian Atlantic Current
NCC	Norwegian Coastal Current
NEMO	Nucleus for European Modelling of the Ocean
NERSC	Nansen Environmental and Remote Sensing Center
neXtSIM	neXt generation Sea Ice Model
NORA3	NOrwegian ReAnalysis 3 km
NPD	Norwegian Petroleum Directorate
NSIDC	National Snow and Ice Data Center
NSR	Northern Sea Route
NtCC	North Cape Current
OILBRICE	OIl spill in Broken Ice
OILMAP	OIL and Spill Impact MAPping
Oil-MARS	Oil Spill Model for the Arctic Seas
OSI-SAF	Ocean and Sea Ice Satellite Application Facility
RIOPS	Regional Ice and Ocean Prediction System
ROMS	Regional Ocean Modeling System
SIMAP	Spill Impact Model Application
SIZEX	Seasonal Ice Zone Experiment
SODA	Simple Ocean Data Assimilation
SVIM	Nordic Seas 4 km numerical ocean model hindcast archive
TOPAZ	Towards an Operational Prediction system for the North Atlantic European coastal Zones
YOPP	Year of Polar Prediction

CRediT authorship contribution statement

Victor de Aguiar: Conceptualization, Methodology, Software, Formal analysis, Investigation, Writing – original draft, Writing – review & editing. **Knut-Frode Dagestad:** Software, Validation, Data curation, Writing – original draft, Writing – review & editing. **Lars Robert Hole:** Writing – original draft, Writing – review & editing, Funding acquisition, Supervision. **Knut Barthel:** Writing – original draft, Writing – review & editing, Supervision.

Declaration of competing interest

The authors have no affiliation with any organization with a direct or indirect financial interest in the subject matter discussed in the manuscript

Acknowledgments

The authors are thankful for the jointly funding provided by the Norwegian Research Council through the Nansen Legacy (project no 276730) and the Fram Centre through the MIKON OSMICO project. Hole was partly funded by the POPCORN project sponsored by the Northern Periphery and Arctic Programme of the European Union. We would like to express our great appreciation to Dr. Wendy Ermold and Dr. Jennifer Hutchings for their constructive assistance provided during the processing of the IABP data. We also thank the reviewers and editors for their constructive suggestions that have greatly improved this work.

References

Afenyo, M., Veitch, B., Khan, F., 2016. A state-of-the-art review of fate and transport of oil spills in open and ice-covered water. Ocean Engineering 119, 233–248. https://doi.org/10.1016/j.oceaneng.2015.10.014. URL: doi:10.3402/polar.v10i1.6723. doi:10.3402/polar.v10i1.6723. https://www.sciencedirect.com/science/article/pii/S002980181500551X.

Ambjorn, C., 2008. Seatrack web forecasts and backtracking of oil spills – an efficient tool to find illegal spills using ais. In: 2008 IEEE/OES US/EU-Baltic International Symposium, pp. 1–9. https://doi.org/10.1109/BALTIC.2008.4625512.

Androulidakis, Y., Kourafalou, V., Hole, L., Le Hénaff, M., Kang, H., 2020. Pathways of oil spills from potential cuban offshore exploration: influence of ocean circulation. Journal of Marine Science and Engineering 8, 1–32. https://doi.org/10.3390/jmse8070535. https://www.mdpi.com/2077-1312/8/7/535.

Arneborg, L., Höglund, A., Axell, L., Lensu, M., Liungman, O., Mattsson, J., 2017. Oil drift modeling in pack ice – sensitivity to oil-in-ice parameters. Ocean Engineering 144, 340–350. https://doi.org/10.1016/j.oceaneng.2017.09.041. http://www.sciencedirect.com/science/article/pii/S0029801817305607.

Beegle-Krause, C., Nordam, T., Reed, M., Daae, R., 2017. State-of-the-art oil spill trajectory prediction in ice infested waters: A journey from high resolution arctic-wide satellite data to advanced oil spill trajectory modeling-what you need to know. In: International Oil Spill Conference Proceedings, 1, pp. 1507–1522. https://doi.org/10.7901/2169-3358-2017.1.1507.

Breivik, Ø., Bidlot, J.-R., Janssen, P.A., 2016. A Stokes drift approximation based on the Phillips spectrum. Ocean Modelling 100, 49–56. https://doi.org/10.1016/j.ocemod.2016.01.005. https://www.sciencedirect.com/science/article/pii/S1463500316000159.

Brekke, C., Espeseth, M., Dagestad, K.-F., Röhrs, J., Hole, L., Reigber, A., 2021. Integrated analysis of multisensor datasets and oil drift simulations — A free-floating oil experiment in the open ocean. Journal of Geophysical Research: Oceans 126, e2020JC016499. https://doi.org/10.1029/2020JC016499.

Buist, I., Potter, S., Trudel, B., Shelnutt, S., Walker, A., Scholz, D., Brandvik, P., Fritt-Rasmussen, J., Allen, A., Smith, P., 2013. In-situ Burning in Ice-affected Waters: State of Knowledge Report. Final Report.

Canada's Oil &amp, Natural Gas Producers, 2018. 2018 Economic Report Series; Canada's Role in the World's Future Energy Mix. Online. https://www.capp.ca/wp-content/uploads/2019/11/2018_Economic_Report_Series_Canada_s_Role_in_the_World_s_Future_Energy_Mix-317291.pdf. (Accessed 19 October 2020).

Carpenter, A., 2019. Oil pollution in the north sea: the impact of governance measures on oil pollution over several decades. Hydrobiologia 845, 109–127. https://doi.org/10.1007/s10750-018-3559-2.

Casati, B., Robinson, T., Lemay, F., Milbrandt, J., Smith, G., Mekis, E., Lespinas, F., Fortin, V., Koltzow, M., Haiden, T., 2021. Performance of the Canadian deterministic prediction systems over the Arctic during the winter and summer. In: YOPP Special Observing Periods. Manuscript in preparation.

Cheng, S., Aydoğdu, A., Rampal, P., Carrassi, A., Bertino, L., 2020. Probabilistic forecasts of sea ice trajectories in the Arctic: impact of uncertainties in surface wind and ice cohesion. Oceans 1, 326–342. https://doi.org/10.3390/oceans1040022. https://www.mdpi.com/2673-1924/1/4/22.

Chikhar, K., Lemieux, J.-F., Dupont, F., Roy, F., Smith, G.C., Brady, M., Howell, S.E.L., Beaini, R., 2019. Sensitivity of ice drift to form drag and ice strength parameterization in a coupled ice–ocean model. Atmosphere-Ocean 57, 329–349. https://doi.org/10.1080/07055900.2019.1694859 doi:10.1080/07055900.2019.1694859. arXiv:doi:10.1080/07055900.2019.1694859.

Copernicus Marine Environment Monitoring Service, 2018. Ocean Products. Online. https://resources.marine.copernicus.eu/?option=com_csw&task=results. (Accessed 19 November 2020).

Corporation, Vectornav, 2019. Vn100 Product Specification. https://www.vectornav.com/docs/default-source/documentation/vn-100-documentation/PB-12-0002.pdf?sfvrsn=9f9fe6b9_18. (Accessed 20 December 2018).

Cox, J.C., Schultz, L.A., 1981. The containment of oil spilled under rough ice. In: International Oil Spill Conference Proceedings, 1, pp. 203–208. https://doi.org/10.7901/2169-3358-1981-1-203 doi:10.7901/2169-3358-1981-1-203. doi:10.7901/2169-3358-1981-1-203. arXiv.

Dagestad, K.-F., Röhrs, J., 2019. Prediction of ocean surface trajectories using satellite derived vs. modeled ocean currents. Remote Sensing of Environment 223, 130–142. https://doi.org/10.1016/j.rse.2019.01.001. https://www.sciencedirect.com/science/article/pii/S003442571930001X.

Dagestad, K.-F., Röhrs, J., Breivik, Ø., Ådlandsvik, B., 2018. Opendrift v1.0: a generic framework for trajectory modelling. In: Geoscientific Model Development, 11, pp. 1405–1420. https://doi.org/10.5194/gmd-11-1405-2018. https://www.geosci-model-dev.net/11/1405/2018/.

Dai, H.-J., McWilliams, J.C., Liang, J.-H., 2019. Wave-driven mesoscale currents in a marginal ice zone. Ocean Modelling 134, 1–17. https://doi.org/10.1016/j.ocemod.2018.11.006. https://www.sciencedirect.com/science/article/pii/S1463500318303810.

Dansereau, V., Weiss, J., Saramito, P., Lattes, P., 2016. A Maxwell Elasto-Brittle rheology for sea ice modelling. The Cryosphere 10, 1339–1359. https://doi.org/10.5194/tc-10-1339-2016. https://tc.copernicus.org/articles/10/1339/2016/.

Directorate, The Norwegian Petroleum, 2018. Resource Report Exploration 2018. Online Technical Report NPD Norway. https://www.npd.no/globalassets/engelsk/3-publications/resource-report/resource-report-2018/hele-rapporten-engelsk.pdf.

Drozdowski, A., Nudds, S., Hannah, C., Niu, H., Peterson, I., Perrie, W., 2011. Review of Oil Spill Trajectory Modelling in the Presence of Ice.

Dupont, F., Higginson, S., Bourdallé-Badie, R., Lu, Y., Roy, F., Smith, G.C., Lemieux, J.-F., Garric, G., Davidson, F., 2015. A high-resolution ocean and sea-ice modelling system for the Arctic and North Atlantic oceans. Geoscientific Model Development 8, 1577–1594. https://doi.org/10.5194/gmd-8-1577-2015. https://gmd.copernicus.org/articles/8/1577/2015/.

Enhancing oil spill response capability in the Baltic Sea Region, 2019. OIL SPILL. Online. https://blogit.utu.fi/oilspill/about-the-project/. (Accessed 11 September 2021).

Faksness, L.-G., Brandvik, P.J., Daae, R.L., Leirvik, F., Børseth, J.F., 2011. Large-scale oil-in-ice experiment in the Barents Sea: monitoring of oil in water and MetOcean interactions. Marine Pollution Bulletin 62, 976–984. https://doi.org/10.1016/j.marpolbul.2011.02.039. https://www.sciencedirect.com/science/article/pii/S0025326X1100110X.

Feltham, D., 2005. Granular flow in the marginal ice zone. Philosophical Transactions of the Royal Society A: Mathematical, Physical and Engineering Sciences 363, 1677–1700. https://doi.org/10.1098/rsta.2005.1601 arXiv:https://royalsocietypublishing.org/doi/pdf/10.1098/rsta.2005.1601. https://royalsocietypublishing.org/doi/abs/10.1098/rsta.2005.1601.

Feltham, D.L., 2008. In: Sea Ice Rheology. Annual Review of Fluid Mechanics, 40, pp. 91–112. https://doi.org/10.1146/annurev.fluid.40.111406.102151.

Fingas, M., Hollebone, B., 2014. In: Oil Behaviour in Ice-Infested Waters. International Oil Spill Conference Proceedings, 2014, pp. 1239–1250. https://doi.org/10.7901/2169-3358-2014.1.1239. https://meridian.allenpress.com/iosc/article-pdf/2014/1/1239/1753817/2169-3358-2014.

Forum, Faglig, 2019. Særlig verdifulle og sårbare områder – faggrunnlag for revisjon og oppdatering av forvaltningsplanene for norske havområder m-1303/2019. https://www.miljodirektoratet.no/globalassets/publikasjoner/m1303/m1303.pdf.

French-McCay, D., Tajalli-Bakhsh, T., Jayko, K., Spaulding, M., Li, Z., 2018. Validation of oil spill transport and fate modeling in Arctic ice. Arctic Science 4, 71–97. https://doi.org/10.1139/as-2017-0027 doi:10.1139/as-2017-0027. doi:10.1139/as-2017-0027.

Furnans, J., Hodges, B., Imberger, J., 2020. State of Energy Report. Online Technical Report Austin, Texas, USA doi:10.1080/07055900.2019.1694859. arXiv:doi:10.1080/07055900.2019.1694859. http://tipro.org/index.php?option=com_content&view=article&id=268.

Gammelsrød, T., Leikvin, Ø., Lien, V., Budgell, W., Loeng, H., Maslowski, W., 2009. Mass and heat transports in the NE Barents Sea: observations and models. Online Journal of Marine Systems 75, 56–69. https://doi.org/10.1016/j.jmarsys.2008.07.010. https://www.sciencedirect.com/science/article/pii/S0924796308001401.

Gearon, M., French-McCay, D., Chaite, E., Zamorski, S., Reich, D., Rowe, J., Schmidt-Etkin, D., 2014. Simap modelling of hypothetical oil spills in the Beaufort Sea for World Wildlife Fund (WWF). In: Summary Report World Wildlife Foundation.

Gjevik, B., Nøst, E., Straume, T., 1994. Model simulations of the tides in the Barents Sea. Journal of Geophysical Research: Oceans 99, 3337–3350. https://doi.org/10.1029/93JC02743. https://agupubs.onlinelibrary.wiley.com/doi/pdf/10.1029/93JC02743.

Haakenstad, H., Breivik, Ø., Furevik, B.R., Reistad, M., Bohlinger, P., Aarsnes, O.J., 2021. NORA3: a nonhydrostatic high-resolution hindcast for the North Sea, the Norwegian Sea and the Barents Sea. Journal of Applied Meteorology and Climatology 60 (10), 1443–1464. https://doi.org/10.1175/JAMC-D-21-0029.1. https://journals.ametsoc.org/view/journals/apme/60/10/JAMC-D-21-0029.1.xml.

Hansen, C., Drinkwater, K., Jähkel, A., Fulton, E., Gorton, R., Skern-Mauritzen, M., 2019. Sensitivity of the norwegian and Barents Sea Atlantis end-to-end ecosystem model to parameter perturbations of key species. Plos One 14, 1–24. https://doi.org/10.1371/journal.pone.0210419. URL: doi:10.1371/journal.pone.0210419.

Heorton, H., Feltham, D., Hunt, J., 2014. The response of the sea ice edge to atmospheric and oceanic jet formation. URL: https://agupubs.onlinelibrary.wiley.com/doi/abs/10.1002/2016JC012113 Journal of Physical Oceanography 44, 2292–2316. https://doi.org/10.1175/JPO-D-13-0184.1. https://journals.ametsoc.org/view/journals/phoc/44/9/jpo-d-13-0184.1.xml.

Hole, L., Dagestad, K.-F., Röhrs, J., Wettre, C., Kourafalou, V., Androulidakis, Y., Kang, H., Le Hénaff, M., Garcia-Pineda, O., 2019. The deepwater horizon oil slick: simulations of river front effects and oil droplet size distribution. J. Mar. Sci. Eng. 7, 1–20. https://doi.org/10.3390/jmse7100329.

Hole, L., de Aguiar, V., Dagestad, K.-F., Kourafalou, V., Androulidakis, Y., Kang, H., Le Hénaff, M., Calzada, A., 2021. Long term simulations of potential oil spills around cuba. Marine Pollution Bulletin 167, 112285. https://doi.org/10.1016/j.marpolbul.2021.112285 doi:10.1080/07055900.2019.1694859. arXiv:doi:10.1080/07055900.2019.1694859. https://www.sciencedirect.com/science/article/pii/S0025326X21003192.

Hunke, E.C., Dukowicz, J.K., 1997. An elastic–viscous–plastic model for sea ice dynamics. Journal of Physical Oceanography 27, 1849–1867. https://doi.org/10.1175/1520-0485(1997)027<1849:AEVPMF>2.0.CO;2 arXiv:https://

royalsocietypublishing.org/doi/pdf/10.1098/rsta.2005.1601. https://journals.ametsoc.org/view/journals/phoc/27/9/1520-0485_1997_027_1849_aevpmf_2.0.co_2.xml.

Huserbråten, M., Eriksen, E., Gjøsæter, H., Vikebø, F., 2019. Polar cod in jeopardy under the retreating Arctic Sea ice. Commun. Biol. 2, 407. https://doi.org/10.1038/s42003-019-0649-2.

Informatics, R.G.C.Risk, 2012. Modeling of potential oil spill behavior when operating Prirazlomnaya OIFP - Assessment of possible oil spill emergency response. In: Technical Report Wild World Foundation (WWF).

Johannessen, O.M., Johannessen, J.A., Morison, J., Farrelly, B.A., Svendsen, E.A.S., 1983. Oceanographic conditions in the marginal ice zone north of Svalbard in early fall 1979 with an emphasis on mesoscale processes. https://agupubs.onlinelibrary.wiley.com/doi/abs/10.1029/JC088iC05p02755 Journal of Geophysical Research: Oceans 88, 2755–2769. https://doi.org/10.1029/JC088iC05p02755. https://agupubs.onlinelibrary.wiley.com/doi/pdf/10.1029/JC088iC05p02755.

Johannessen, J., Johannessen, O., Svendsen, E., Shuchman, R., Manley, T., Campbell, W., Josberger, E., Sandven, S., Gascard, J., Olaussen, T., Davidson, K., Van Leer, J., 1987. Mesoscale eddies in the Fram Strait marginal ice zone during the 1983 and 1984 Marginal Ice Zone experiments. J. Geophys. Res. 92, 6754–6772. https://doi.org/10.1080/1755876X.2021.1883293.

Johannessen, O.M., Sagen, H., Nesse, Ø., Engelsen, I., Sanvend, S., 1992. Ambient noise generation by ice-ocean jets, eddies and tidal current in the marginal ice zone. In: Weydert, M. (Ed.), European Conference on Underwater Acoustics. Elsevier Applied Science, pp. 28–38.

Jones, C., Dagestad, K.-F., Breivik, Ø., Holt, B., Röhrs, J., Christensen, K., Espeseth, M., Brekke, C., Skrunes, S., 2016. Measurement and modeling of oil slick transport. URL: https://agupubs.onlinelibrary.wiley.com/doi/abs/10.1002/2016JC012113 Journal of Geophysical Research: Oceans 121, 7759–7775. https://doi.org/10.1002/2016JC012113. https://agupubs.onlinelibrary.wiley.com/doi/pdf/10.1002/2016JC012113.

Kostianoy, A., Ambjorn, C., Soloviev, D., 2008. Seatrack web: A numerical tool to protect the baltic sea marine protected areas. In: 2008 IEEE/OES US/EU-Baltic International Symposium, pp. 1–6. https://doi.org/10.1109/BALTIC.2008.4625487.

Kozlov, I., Artamonova, A., Manucharyan, G., Kubryakov, A., 2019. Eddies in the western Arctic ocean from spaceborne SAR observations over open ocean and marginal ice zones. Journal of Geophysical Research: Oceans 124, 6601–6616. https://doi.org/10.1029/2019JC015113. https://agupubs.onlinelibrary.wiley.com/doi/pdf/10.1029/2019JC015113.

Lemieux, J.-F., Beaudoin, C., Dupont, F., Roy, F., Smith, G.C., Shlyaeva, A., Buehner, M., Caya, A., Chen, J., Carrieres, T., Pogson, L., DeRepentigny, P., Plante, A., Pestieau, P., Pellerin, P., Ritchie, H., Garric, G., Ferry, N., 2015. The regional ice prediction system (RIPOS): verification of forecast sea ice concentration. URL: https://rmets.onlinelibrary.wiley.com/doi/abs/10.1002/qj.2526 Quarterly Journal of the Royal Meteorological Society 142, 632–643. https://doi.org/10.1002/qj.2526. https://rmets.onlinelibrary.wiley.com/doi/pdf/10.1002/qj.2526.

Li, Z., Spaulding, M.L., French-McCay, D., 2017. An algorithm for modeling entrainment and naturally and chemically dispersed oil droplet size distribution under surface breaking wave conditions. Marine Pollution Bulletin 119, 145–152. https://doi.org/10.1016/j.marpolbul.2017.03.048. https://www.sciencedirect.com/science/article/pii/S0025326X17302680.

Lien, V., Gusdal, Y., Albretsen, J., Melsom, A., Vikebø, F., 2013. Evaluation of a nordic seas 4 km numerical ocean model hindcast archive (SVIM), 1960–2011. Fisken Og Havet 7, 1–80.

Liu, Y., Weisberg, R., 2011. Evaluation of trajectory modeling in different dynamic regions using normalized cumulative Lagrangian separation. URL: https://agupubs.onlinelibrary.wiley.com/doi/abs/10.1029/2010JC006837 Journal of Geophysical Research: Oceans 116, 1–13. https://doi.org/10.1029/2010JC006837. https://agupubs.onlinelibrary.wiley.com/doi/pdf/10.1029/2010JC006837.

Liu, Y., Weisberg, R., Vignudelli, S., Mitchum, G., 2014. Evaluation of altimetry-derived surface current products using Lagrangian drifter trajectories in the eastern Gulf of Mexico. URL: https://agupubs.onlinelibrary.wiley.com/doi/abs/10.1002/2013JC009710 Journal of Geophysical Research: Oceans 119, 2827–2842. https://doi.org/10.1002/2013JC009710. https://agupubs.onlinelibrary.wiley.com/doi/pdf/10.1002/2013JC009710.

Loeng, H., 1991. Features of the physical oceanographic conditions of the Barents Sea. Polar Research 10, 5–18. https://doi.org/10.3402/polar.v10i1.6723. URL: doi:10.3402/polar.v10i1.6723. doi:10.3402/polar.v10i1.6723.

Lüpkes, C., Gryanik, V., 2015. A stability-dependent parametrization of transfer coefficients for momentum and heat over polar sea ice to be used in climate models. Journal of Geophysical Research: Atmospheres 120, 552–581. https://doi.org/10.1002/2014JD022418.

Marchenko, A., Rabault, J., Sutherland, G., Collins, C., Wadhams, P., Chumakov, M., 2017. Field observations and preliminary investigations of a wave event in solid drift ice in the Barents Sea. In: Proceedings-international Conference on Port and Ocean Engineering Under Arctic Conditions. Port and Ocean Engineering Under Arctic Conditions.

Martin, T., Tsamados, M., Schroeder, D., Feltham, D., 2016. The impact of variable sea ice roughness on changes in Arctic ocean surface stress: a model study. Journal of Geophysical Research: Oceans 121, 1931–1952. https://doi.org/10.1002/2015JC011186.

Monfils, R., 2005. The global risk of marine pollution from WWII shipwrecks: examples from the seven seas. In: International Oil Spill Conference Proceedings, 2005, pp. 1049–1054. https://doi.org/10.7901/2169-3358-2005-1-1049.

Morell Villalonga, M., Espino Infantes, M., Grifoll Colls, M., Mestres Ridge, M., 2020. Environmental management system for the analysis of oil spill risk using probabilistic simulations. application at Tarragona Monobuoy. J. Mar. Sci. Eng. 8. https://www.mdpi.com/2077-1312/8/4/277.

Muench, R., Schumacher, J., 1985. On the Bering Sea ice edge front. Journal of Geophysical Research: Oceans 90, 3185–3197. https://doi.org/10.1029/JC090iC02p03185.

National Snow and Ice Data Center (NSIDC), 2017. Sea Ice Index, Version 3. Monthly Sea Ice Concentration Images, North. Online. https://doi.org/10.7265/N5K072F8. (Accessed 13 July 2020).

Nordam, T., Dunnebier, D., Beegle-Krause, C., Reed, M., Slagstad, D., 2017. Impact of climate change and seasonal trends on the fate of Arctic oil spills. Ambio 46, 442–452. https://doi.org/10.1007/s13280-017-0961-3.

Nordam, T., Beegle-Krause, C., Skancke, J., Nepstad, R., Reed, M., 2019. Improving oil spill trajectory modelling in the Arctic. https://agupubs.onlinelibrary.wiley.com/doi/abs/10.1029/JC088iC05p02755 Marine Pollution Bulletin 140, 65–74. https://doi.org/10.1016/j.marpolbul.2019.01.019. http://www.sciencedirect.com/science/article/pii/S0025326X19300190.

Nordam, T., Nepstad, R., Litzler, E., Röhrs, J., 2019. On the use of random walk schemes in oil spill modelling. Marine Pollution Bulletin 146, 631–638. https://doi.org/10.1016/j.marpolbul.2019.07.002. https://www.sciencedirect.com/science/article/pii/S0025326X19305338.

OSPAR Commission, 2017. Ospar Report on Discharges, Spills and Emissions From Offshore Oil and Gas Installations in 2017. https://www.ospar.org/documents?v=42260.

OSPAR Commission, 2021. Offshore Installations — Webpage. Online. OSPAR Commission. https://www.ospar.org/work-areas/oic/installations. (Accessed 28 May 2021).

Petroleum, British, 2019. Statistical Review of World Energy, 68th edition. In: Technical Report.

Petty, A.A., Tsamados, M.C., Kurtz, N.T., 2017. Atmospheric form drag coefficients over Arctic sea ice using remotely sensed ice topography data, spring 2009–2015. Journal of Geophysical Research: Earth Surface 122, 1472–1490. https://doi.org/10.1002/2017JF004209. https://agupubs.onlinelibrary.wiley.com/doi/abs/10.1002/2017JF004209.

Platov, G., Golubeva, E., 2020. Characteristics of mesoscale eddies of Arctic marginal seas: results of numerical modeling. IOP Conference Series: Earth and Environmental Science 611, 012009. https://doi.org/10.1088/1755-1315/611/1/012009.

Price, J., Reed, M., Howard, M., Johnson, W., Ji, Z.-G., Marshall, C., Guinasso, N., Rainey, G., 2006. Preliminary assessment of an oil-spill trajectory model using satellite-tracked, oil-spill-simulating drifters. Environ. Model. Softw. 21, 258–270. https://doi.org/10.1016/j.envsoft.2004.04.025.

Rabatel, M., Rampal, P., Carrassi, A., Bertino, L., Jones, C.K.R.T., 2018. Impact of rheology on probabilistic forecasts of sea ice trajectories: application for search and rescue operations in the Arctic. Cryosphere 12, 935–953. https://doi.org/10.5194/tc-12-935-2018.

Rabault, J., Sutherland, G., Ward, B., Christensen, K., Halsne, T., Jensen, A., 2016. Measurements of waves in landfast ice using inertial motion units. IEEE Trans. Geosci. Remote Sens. 54, 6399–6408. https://doi.org/10.1109/TGRS.2016.2584182.

Rabault, J., Sutherland, G., Gundersen, O., Jensen, A., 2017. Measurements of wave damping by a grease ice slick in Svalbard using off-the-shelf sensors and open-source electronics. J. Glaciol. 63, 372–381. https://doi.org/10.1017/jog.2017.1.

Rabault, J., Sutherland, G., Gundersen, O., Jensen, A., Marchenko, A., Breivik, Ø., 2020. An open source, versatile, affordable waves in ice instrument for scientific measurements in the polar regions. Cold Regions Science and Technology 170, 102955. https://doi.org/10.1016/j.coldregions.2019.102955. https://www.sciencedirect.com/science/article/pii/S0165232X19300230.

Rampal, P., Bouillon, S., Ólason, E., Morlighem, M., 2016. neXtSIM: a new Lagrangian Sea ice model. Cryosphere 10, 1055–1073. https://doi.org/10.5194/tc-10-1055-2016.

Reed, M., Aamo, O., 1994. Real time oil spill forecasting during an experimental oil spill in the Arctic ice. Spill Science & Technology Bulletin 1, 69–77. https://doi.org/10.1016/1353-2561(94)90009-4. http://www.sciencedirect.com/science/article/pii/1353256194900094.

Reed, M., Johansen, Ø., Brandvik, P., Daling, P., Lewis, A., Fiocco, R., Mackay, D., Prentki, R., 1999. Oil spill modeling towards the close of the 20th century: Overview of the state of the art. Spill Science & Technology Bulletin 5, 3–16. https://doi.org/10.1016/S1353-2561(98)00029-2. http://www.sciencedirect.com/science/article/pii/S1353256198000292.

Röhrs, J., Dagestad, K.-F., Asbjørnsen, H., Nordam, T., Skancke, J., Jones, C.E., Brekke, C., 2018. The effect of vertical mixing on the horizontal drift of oil spills. Ocean Sci. 14, 1581–1601. https://doi.org/10.5194/os-14-1581-2018.

Ross, S., Dickins, D., 1987. Field Research Spills to Investigate the Physical and Chemical Fate of Oil in Pack Ice. https://www.esrfunds.org/sites/www.esrfunds.org/files/publications/ESRF062-SL-Ross-and-DF-Dickens.pdf.

Sakov, P., Counillon, F., Bertino, L., Lisåter, K.A., Oke, P.R., Korablev, A., 2012. TOPAZ4: an ocean-sea ice data assimilation system for the North Atlantic and Arctic. Ocean Sci. 8, 633–656. https://doi.org/10.5194/os-8-633-2012.

Schrum, C., Alekseeva, I., St. John, M., 2006. Development of a coupled physical–biological ecosystem model ECOSMO: Part I: Model description and validation for the North Sea. Journal of Marine Systems 61, 79–99. https://doi.org/10.1016/j.jmarsys.2006.01.005. https://www.sciencedirect.com/science/article/pii/S0924796306000297.

Serreze, M., Holland, M., Stroeve, J., 2007. Perspectives on the arctic's shrinking sea-ice cover. URL: https://science.sciencemag.org/content/315/5818/1533 Science 315, 1533–1536. https://doi.org/10.1126/science.1139426. https://science.sciencemag.org/content/315/5818/1533.full.pdf.

Simonsen, M., Hackett, B., Bertino, L., Rø, L., Waagbø, G., Drivdal, M., Sutherland, G., 2019. Product User Manual For Arctic Ocean Physical and BIO Analysis and Forecasting Products. URL: https://agupubs.onlinelibrary.wiley.com/doi/abs/10.1029/2010JC006837. Copernicus Marine Environment Monitoring Service.

Singsaas, I., Leirvik, F., Daling, P., Guénette, C., Sørheim, K., 2020. Fate and behaviour of weathered oil drifting into sea ice, using a novel wave and current flume. Marine Pollution Bulletin 159, 111485. https://doi.org/10.1016/j.marpolbul.2020.111485. https://www.sciencedirect.com/science/article/pii/S0025326X20306032.

Smith, G., Roy, F., Reszka, M., Surcel Colan, D., He, Z., Deacu, D., Belanger, J.-M., Skachko, S., Liu, Y., Dupont, F., Lemieux, J.-F., Beaudoin, C., Tranchant, B., Drévillon, M., Garric, G., Testut, C.-E., Lellouche, J.-M., Pellerin, P., Ritchie, H., Lu, Y., Davidson, F., Buehner, M., Caya, A., Lajoie, M., 2016. Sea ice forecast verification in the Canadian global ice ocean prediction system. Q. J. R. Meteorol. Soc. 142, 659–671. https://doi.org/10.1002/qj.2555. https://rmets.onlinelibrary.wiley.com/doi/pdf/10.1002/qj.2555.

Solbrekke, I.M., Sorteberg, A., Haakenstad, H., 2021. Norwegian hindcast archive (NORA3) – a validation of offshore wind resources in the North Sea and Norwegian Sea. Wind Energy Science Discussions 2021, 1–31. https://doi.org/10.5194/wes-2021-22. https://wes.copernicus.org/preprints/wes-2021-22/.

Sørstrøm, S., Brandvik, P., Buist, I., Daling, P., Dickins, D., Faksness, L., Potter, S., Fritt-Rasmussen, J., Singsaas, I., 2010. Joint industry program on oil contingency for Arctic and ice-covered waters. In: Summary report SINTEF.

Stanovoy, V., Eremina, T., Isaev, A., Neelov, I., Vankevich, R., Ryabchenko, V., 2012. Modeling of oil spills in ice conditions in the Gulf of Finland on the basis of an operative forecasting system. Okeanologiya 52 (6), 754–759. https://doi.org/10.1134/S0001437012060136.

Sutherland, G., Rabault, J., 2016. Observations of wave dispersion and attenuation in landfast ice. URL: https://agupubs.onlinelibrary.wiley.com/doi/abs/10.1002/2015JC011446 Journal of Geophysical Research: Oceans 121, 1984–1997. https://doi.org/10.1002/2015JC011446. https://agupubs.onlinelibrary.wiley.com/doi/pdf/10.1002/2015JC011446.

The International Tanker Owners Pollution Federation, 2020. Oil Tanker Spill Statistics 2019, Special Edition: 50 Years of Data, 1970 - 2019. Online. https://www.itopf.org/fileadmin/data/Documents/Company_Lit/Oil_Spill_Stats_brochure_2020_for_web.pdf. (Accessed 24 October 2020).

Trites, R., Lawrence, D., Vandermeulen, J., 1986. Modelling oil movements from the Kurdistan spill in Cabot strait, Nova Scotia. Atmosphere-Ocean 24, 253–264.

Tsamados, M., Feltham, D., Schroeder, D., Flocco, D., Farrell, S., Kurtz, N., Laxon, S., Bacon, S., 2014. Impact of variable atmospheric and oceanic form drag on simulations of Arctic sea ice. Journal of Physical Oceanography 44, 1329–1353. https://doi.org/10.1175/JPO-D-13-0215.1. https://journals.ametsoc.org/view/journals/phoc/44/5/jpo-d-13-0215.1.xml.

Venkatesh, S., El-Tahan, H., Comfort, G., Abdelnour, R., 1990. Modelling the behaviour of oil spills in ice-infested waters. Atmosphere-Ocean 28, 303–329.

de Vos, M., Barnes, M., Biddle, L., Swart, S., Ramjukadh, C.-L., Vichi, M., 2021. Evaluating numerical and free-drift forecasts of sea ice drift during a Southern Ocean research expedition: an operational perspective. Journal of operationalOceanography 1–17. https://doi.org/10.1080/1755876X.2021.1883293.

Wadhams, P., Davis, N., 2000. Further evidence of ice thinning in the arctic ocean. Geophysical Research Letters 27, 3973–3975. https://doi.org/10.1029/2000GL011802. https://agupubs.onlinelibrary.wiley.com/doi/pdf/10.1029/2000GL011802.

Wang, Q., Koldunov, N., Danilov, S., Sidorenko, D., Wekerle, C., Scholz, P., Bashmachnikov, I., Jung, T., 2020. Eddy kinetic energy in the Arctic ocean from a global simulation with a 1-km Arctic. URL: https://agupubs.onlinelibrary.wiley.com/doi/abs/10.1002/2015JC011446 Geophysical Research Letters 47, e2020GL088550. https://doi.org/10.1029/2020GL088550. https://agupubs.onlinelibrary.wiley.com/doi/pdf/10.1029/2020GL088550.E2020GL088550.

Wassmann, P., Reigstad, M., Haug, T., Rudels, B., Carroll, M., Hop, H., Gabrielsen, G., Falk-Petersen, S., Denisenko, S., Arashkevich, E., Slagstad, D., Pavlova, O., 2006. Food webs and carbon ux in the Barents Sea. Progress in Oceanography 71, 232–287. https://doi.org/10.1016/j.pocean.2006.10.003. Structure and function of contemporary food webs on Arctic shelves: a pan-Arctic comparison. https://www.sciencedirect.com/science/article/pii/S0079661106001315.

Wekerle, C., Hattermann, T., Wang, Q., Crews, L., von Appen, W.-J., Danilov, S., 2020. Properties and dynamics of mesoscale eddies in Fram Strait from a comparison between two high-resolution ocean–sea ice models. Ocean Sci. 16, 1225–1246. https://doi.org/10.5194/os-16-1225-2020. https://os.copernicus.org/articles/16/1225/2020/.

Wilkinson, J., Beegle-Krause, C., Evers, K., Hughes, N., Lewis, A., Reed, M., Wadhams, P., 2017. Oil spill response capabilities and technologies for ice-covered Arctic marine waters: a review of recent developments and established practices. Ambio 93, 423–441. https://doi.org/10.1007/s13280-017-0958-y.

Willmott, C., 1981. On the vaidation of models. Phys. Geogr. 2, 184–194. https://doi.org/10.1080/02723646.1981.10642213.

Xie, J., Bertino, L., 2021. Quality Information Document - Arctic Physical Multi Year Product ARCTIC MULTIYEAR PHY 002 003. Copernicus Marine Environment Monitoring Service.

Zhang, X., Cheng, L., Zhang, F., Wu, J., Li, S., Liu, J., Chu, S., Xia, N., Min, K., Zuo, X., Li, M., 2020. Evaluation of multi-source forcing datasets for drift trajectory prediction using Lagrangian models in the South China Sea. Applied Ocean Research 104, 102395. https://doi.org/10.1016/j.apor.2020.102395. https://www.sciencedirect.com/science/article/pii/S0141118720309548.